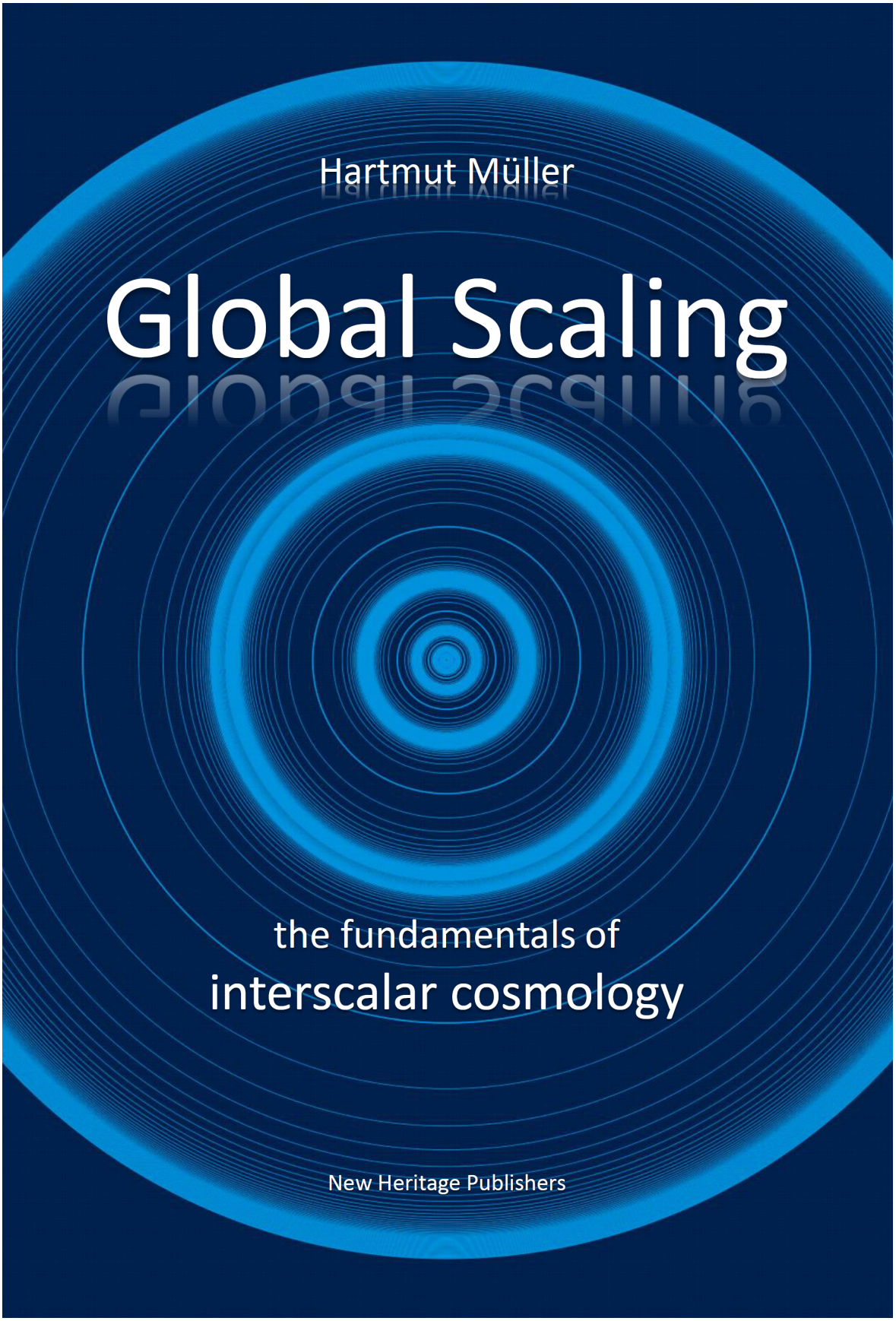
Hartmut Müller
Global Scaling
the fundamentals of
interscalar cosmology
New Heritage Publishers

New Heritage Publishers

Hartmut Müller

GLOBAL SCALING

the fundamentals of interscalar cosmology

Brooklyn, New York, USA
— 2018 —

This book was typeset using the LaTeX typesetting system.

ISBN 978-0-9981894-0-6

New Heritage Publishers
Brooklyn, New York, USA

Content

Editorial Foreword

Each fundamental scientific discovery that changed Humanity's views of the world did not appear out of nowhere but was built on the "shoulders" of the giants of science from before. This is also true for Global Scaling authored by Hartmut Müller.

The natural philosophers of ancient Greece already pointed out that all of physical reality is created according to a harmonic hierarchy which seems to be valid for the full range of physical scales, from the very small particles of substance to the universe as a whole.

In the 1950s, Kyril Dombrowski (1913–1997), a mathematician and optical engineer, discovered how the minima and maxima in the rational number distributions determine various resonance phenomena such as the distribution of the orbits of planets and the electrons in the atom.

Benoit Mandelbrot (1924–2010), one of the great mathematicians of the 20th century, discovered in the 1970s the key role fractal sets play in the organisation of physical reality. Julia and Mandelbrot Sets show endless repetitions of their fragments throughout all the complete range of physical scales. Mandelbrot called it the fractal geometry of nature.

Hartmut Müller continued this line of research in the 1980s. He developed the concept of Global Scaling, a theory based on the properties of rational and transcendental numbers and continued fractions. It explains how the distributions of numbers are not only responsible for the structure of matter but also the dynamics of the physical, biological and social phenomena.

Applications of Müller's Global Scaling are so manifold and varied that they cover all known fields of science from mathematics, physics, and astronomy to biology, political science and economics. In this book, many of the possible fundamental applications of Global Scaling can only be briefly outlined and will require further detailed study, while its main focus is placed on examples from physics and astronomy — the structure of matter — as the professional fields of the author.

This small book is designed to be studied for years to come. We are convinced that after reading it many young people will come to explore the fundamentals of science. This book is truly a stimulus of thought for future generations of research.

We are greatly honoured to be editors of this book. And it is our duty as scientists to support this research and its author.

Pushchino, July 12, 2018 Dmitri Rabounski and Simon Shnoll

Preface

The time will come when
all people will see as I do.

Giordano Bruno

I welcome you to the book for thinking, curious, courageous and honest people! So it might not be interesting to everyone.

But anyone looking at the world with an inquisitive mind will not regret following me to experience the spirit of exploration of the universe in a way that few have done before! If, for most of your life, you have searched for certain answers, you may actually find them here...

I can promise that reading this book will not be a waste of your time. It is the experience of a discovery that I want to share with you.

Sit back and enjoy the ride...

Valle del Sole, July 1, 2018 Hartmut Müller

Many Questions — No Answer

Did you ever ask yourself why the universe is so big? Forty thousand billion kilometers[1] to the neighboring Alpha Centauri system, two million light years to the Andromeda galaxy! And, did you ever ask why the universe is so small? A thousandth of a millimeter for a living cell, a ten-millionth of a millimeter for a whole atom!

If you do not know the answers, you don't need to be ashamed. Even modern science has no plausible explanation. And, this is not an exception, but rather a typical situation. Always when science can't answer simple questions, some new paradigm rises at the scientific horizon.

There are so many questions without answer, you do not believe that? Here are some of them:

- Why is the normal resting heart rate for adults close to one beat per second and the breathing rate close to 15 breaths per minute?
- Why does the electrical Theta activity of the brain range between 3 and 7 Hz, the Alpha activity between 8 and 13 Hz and the Beta activity between 14 and 34 Hz?
- Why is the adult human brain mass close to 1.4 kg?
- Why does the hypophysis gland weight 500 mg?
- Why is the wavelength 280 nm dividing ultraviolet B and C light?
- Why is the average temperature of the cosmic microwave background radiation 2.725 K?
- Why have the Sun and the Moon, the gas giant Jupiter and the planetoid Ceres, but also Earth and Mars similar rotation periods?
- Why have different planets as Venus and Uranus, as well as Mars and Mercury similar surface gravity accelerations?
- Why have several planets in the Trappist 1 system the same orbital periods as the moons of Jupiter, Saturn and Uranus?

There are many more questions like these — there are thousands. That's no joke. And all these questions are not even topics of theoretical research, because in the current paradigm of science, they are considered to be accidental.

Perhaps you will ask now — how can it be that so many questions remain unanswered while science is dealing with black holes and dark matter?

[1] Forty thousand billion kilometers are 4.3 light years.

A very good question. First, the emergence of highly speculative, non-measurable entities and their exploration is a typical feature of a conceptual crisis in natural science and a strong indicator of an upcoming profound paradigm shift. Secondly, the emergence of those entities is a sign of psychological repression, whereby real facts are excluded from the conscious perception and substituted by exotic and surrealistic ideas which convince you that it is vital to know how you can exit a black hole after it has eaten you.

By the way, did you notice something that they have in common while reading the example questions above?

Well, all the questions are about concrete measurements. And that is precisely what today's paradigm lacks. Known laws of nature describe how one quantity changes in dependency on another. For example, Kepler's third law describes how the orbital period of a planet changes with its orbital distance. However, Kepler's law cannot explain why the solar system has established Jupiter's orbital period at 11.86 years and not 10.27 or 14.69 years. Even Newton's gravitational law or Einstein's theory of relativity cannot explain this. And this isn't just a shortcoming of astrophysics only.

In biophysics, Kleiber's law describes how metabolic rates in mammals depend on the body mass. The law affirms that larger-bodied species like elephants have lower mass-specific metabolic rates and lower heart rates, compared to smaller-bodied species like mice. However, currently there is no law known that could explain why billions of adults of the species Homo sapiens prefer to have a heart rate of $60-70$ beats per minute and a breathing rate of $12-17$ breaths per minute. Furthermore, currently there is no law known that could explain why brain oscillations of the Alpha type range between 8 and 13 Hz, of the Beta type between 14 and 34 Hz, why all mammals have these brain frequency ranges in common and why they coincide with Schumann-resonances.

Reading this book, you will find reasonable and precise answers to all these and many other questions. You will also see that all these questions have a common origin and therefore a common explanation.

Now you are going to make an amazing discovery and I'm happy to accompany you! It feels like I was going to make this experience again and I envy you for the moment of a pure rush of adrenaline that awaits you and may change your life forever.

The Power of Euler's Number

> If you want to find the secrets of the universe,
> think in terms of frequency and vibration.
>
> *Nikola Tesla*

Ok let's get started. Talking about measurement[1], it results always in a number that is the ratio of two physical quantities where one of them is the reference quantity called unit of measurement. For example, 0.615 years, the orbital period of Venus. In this case, the orbital period of the Earth (one year) is the unit of measurement. Therefore, the number 0.615 is the Venus-to-Earth orbital period ratio.

If this ratio were equal 1/2 or 2/3, then Venus' orbital movement would be in resonance with that of the Earth. In that case, periodic interaction could progressively rock the orbital movement of both planets and ultimately cause a resonance disaster that could destabilize the whole solar system. Therefore, the solar system can establish only those orbits which avoid whole number ratios.

In mathematics, ratios of whole numbers are called rational numbers. For example, 2/3 (two-thirds) is a rational number. Besides rational numbers, there are also irrational numbers. They cannot be represented as a ratio of whole numbers and consequently, they should not cause destabilizing resonance interaction.[2]

For example, the square root of two $\sqrt{2} = 1.414\ldots$ or the golden number $\phi = (\sqrt{5}+1)/2 = 1.618\ldots$ are irrational numbers. Several authors[3] have suggested that the Venus-to-Earth orbital period ratio 0.615 corresponds with the reciprocal golden number $1/\phi = 1/1.618\ldots = 0.618\ldots$

With reference to the solar system we may therefore expect that if the ratio of two orbital periods is not rational but, for example equals

---

[1] International Vocabulary of Metrology — Basic and General Concepts and Associated Terms. International Bureau of Weights and Measures, 2008.

[2] Dombrowski K. Rational Numbers Distribution and Resonance. *Progress in Physics*, issue 1, 65–67, 2005.

[3] Pletser V. Orbital Period Ratios and Fibonacci Numbers in Solar Planetary and Satellite Systems and in Exoplanetary Systems. arXiv:1803.02828 (2018); Butusov K. P. The Golden Ratio in the solar system. *Problems of Cosmological Research*, vol. 7, Moscow–Leningrad, 1978.

ϕ, the orbital movements should not have resonance interaction and should not destabilize the system.

Nevertheless, even this irrational ratio can cause a resonance disaster, because according to the third law of Kepler, the cube of the orbital distance is proportional to the square of the orbital period. Indeed, the square of $\sqrt{2}$ returns the whole number 2. Even the square of the golden number ϕ returns the whole number 5 after its multiplication by 2 and removal of 1.

This is why roots of whole numbers, even being irrational, cannot guarantee that resonance interaction will be avoided concerning all physical quantities of the system.

Fortunately, there is another type of irrational numbers called transcendental which are not roots of whole or rational numbers. They cannot be transformed into rational or whole numbers by addition or multiplication and consequently, they should never provide resonance interaction.

Indeed, planets are changing their position in space continuously. This temporal change of the position in space is described by the velocity, a quantity called derivative. The derivative of a quantity is its instantaneous rate of change.

Actually, the orbital velocity isn't constant either, but increases and decreases with the change of the orbital distance. This temporal change of the velocity is described by an acceleration, a derivative of the velocity. Naturally, the acceleration isn't constant either.

If you ask me now if there is any real transcendental function that inhibits resonance interaction also regarding velocities, accelerations and other derivatives, I can give you a very positive answer. Yes, there is one, but only one solution: it is the natural exponential function e^x, because it is the only function that is the derivative of itself:

$$\frac{d}{dx}\, e^x = e^x$$

For $x = 1$ the natural exponential function e^x gives Euler's number $e = 2.71828\ldots$ [1]

Consequently, so long as the ratio of physical quantities is given by the natural exponential function e^x, the ratios of their derivatives will be also given by the natural exponential function e^x, so that the system remains stable even when quantities are changing. And this is valid for any system, regardless of its complexity, because of the unique arithmetic properties of Euler's transcendental number $e = 2.71828\ldots$

[1] Maor E. *e*: The Story of a Number. Princeton University Press, 1994.

As we can see, the classification of real numbers, in particular the difference between rational, irrational and transcendental numbers is not only a mathematical task. It is also an essential aspect of stability in complex systems.[1]

Now let's come back to our initial example of the orbital period of Venus. How can we find out if the Venus-to-Earth orbital period ratio is a rational, irrational or transcendental number?

Judging from the first impression, the obtained value 0.615 seems to be a rational number, because it has a finite number of digits and can be presented as a ratio of whole numbers: $0.615 = 123/200$. On the other hand, the circumstance that the number of digits is finite, could be also a consequence of limited precision of measurement. In fact, higher resolution data[2] deliver more digits, for example 0.615198 years = 224.701 days = 224 days, 16 hours and 49 minutes. Indeed, also this value is only an average.

In reality, the sidereal orbital period of Venus is not constant, but varies between 224.695 days = 0.615181 years and 224.709 days = 0.615220 years. According to classic models, that's due to perturbations from other planets, mainly Jupiter and Earth. Usually the uncertainty is put in brackets so we can approximately write 0.61520(2) years for the sidereal orbital period of Venus.

Let's take another example. In 1990, the worldwide best measurements[3] of the proton-to-electron mass ratio delivered the value 1836.152701(37). In 2017, the value 1836.15267389(17) was obtained. As you can see, not only the resolution is improved by two digits, but also the values of some lower digits are changed. Nevertheless, the 2017 measurements do not contradict the 1990 ones, because the limits of the 2017 measurements are within the 1990 limits, confirming the hypothesis about constancy of the proton-to-electron mass ratio.

Now you can understand that it is not so simple to clarify the type of number a measured ratio corresponds to. In general, there is no possibility to know it for sure. However, considering the finite resolution of any measurement, we can state that any obtained value is always an approximation and it is very important to know the amount of its uncertainty.

It is remarkable that approximation interconnects all types of real numbers — rational, irrational algebraic and transcendental. In 1950,

[1] Panchelyuga V. A., Panchelyuga M. S. Resonance and Fractals on the Real Numbers Set. *Progress in Physics*, issue 4, 48–53, 2012.

[2] Venus Fact Sheet. NASA Space Science Archive. www.nssdc.gsfc.nasa.gov

[3] Particle Data Group. www.pdg.lbl.gov

the mathematician Khinchin[1] made a very important discovery: He could demonstrate that continued fractions deliver biunique (one-to-one) representations of all real numbers, rational and irrational. Whereas infinite continued fractions represent irrational numbers, finite continued fractions represent always rational numbers. In this way, any irrational number can be approximated by finite continued fractions, which are the convergents and deliver always the nearest and quickest rational approximation.

It is notable that the best rational approximation of an irrational number by a finite continued fraction is not a task of computation, but only an act of termination of the fractal recursion. For example, the golden number $\phi = (\sqrt{5}+1)/2 = 1.618\ldots$ has a biunique representation as simple continued fraction:

$$\phi = 1 + \cfrac{1}{1 + \cfrac{1}{1 + \cfrac{1}{1 + \cdots}}}$$

To save space, in the following we use square brackets to write down continued fractions, for example the golden number $\phi = [1;\ 1,\ 1,\ \ldots]$. As you can see, it contains only the number 1. So long as the sequence of denominators is considered as infinite, this continued fraction represents the irrational number ϕ. If only you truncate the continued fraction, the sequence of denominators will be finite and you get a convergent that is always the nearest rational approximation of the irrational number ϕ.

Let's see how it works. Increasing always the length of the continued fraction, we obtain the following sequence of rational approximations of ϕ, from the worst to always better and better ones:

$[1] = 1$
$[1;\ 1] = 2$
$[1;\ 1,\ 1] = 3/2 = 1.5$
$[1;\ 1,\ 1,\ 1] = 5/3 = 1.\overline{66}$
$[1;\ 1,\ 1,\ 1,\ 1] = 8/5 = 1.6$
$[1;\ 1,\ 1,\ 1,\ 1,\ 1] = 13/8 = 1.625$
$[1;\ 1,\ 1,\ 1,\ 1,\ 1,\ 1] = 21/13 = 1.\overline{615384}$
$[1;\ 1,\ 1,\ 1,\ 1,\ 1,\ 1,\ 1] = 34/21 = 1.\overline{619047}$
$[1;\ 1,\ 1,\ 1,\ 1,\ 1,\ 1,\ 1,\ 1] = 55/34 = 1.617\overline{64705882352941 17}$
$[1;\ 1,\ 1,\ 1,\ 1,\ 1,\ 1,\ 1,\ 1,\ 1] = 89/55 = 1.\overline{618}$

[1] Khintchine A. Continued fractions. University of Chicago Press, Chicago, 1964.

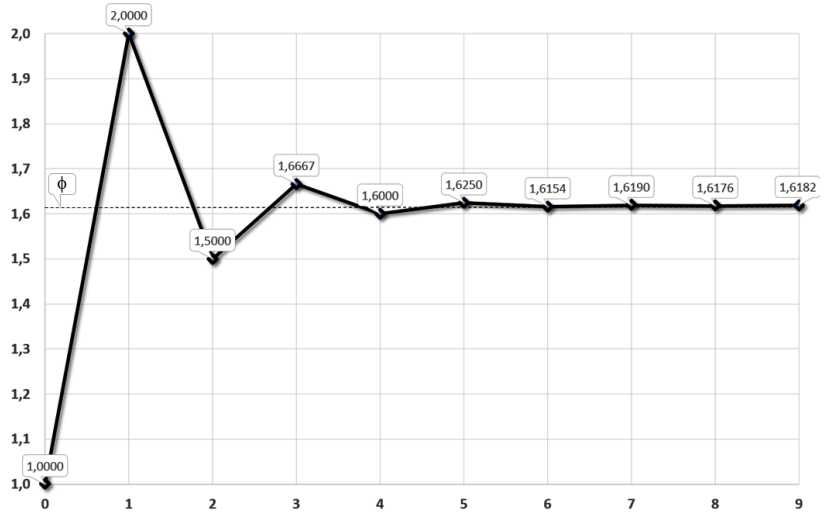

Figure 1: The approximation steps $0-9$ of the golden number $\phi = 1.618\ldots$ (dotted line) by continued fraction.

Figure 1 demonstrates the process of step by step approximation. As you can see, the rational approximations oscillate around the eigenvalue ϕ of the continued fraction that is shown as dotted line. With every step the approximation comes closer and closer to ϕ, never reaching it and describing a damped asymptotic oscillation around ϕ.

By the way, in 1950 Gantmacher and Krein[1] have demonstrated that continued fractions are solutions of the Euler-Lagrange equation for low amplitude harmonic oscillations in simple chain systems. Terskich[2] generalized this method for the analysis of oscillations in branched chain systems. The continued fraction method can also be extended to the analysis of chain systems of harmonic quantum oscillators.[3]

The rational approximations of the golden number ϕ are always ratios of neighboring Fibonacci numbers — the elements of the recursive sequence 1, 1, 2, 3, 5, 8, 13, ... where the sum of two neighbors always yields the following number[4].

[1] Gantmacher F. R., Krein M. G. Oscillation matrixes, oscillation cores and low oscillations of mechanical systems. Leningrad, 1950.

[2] Terskich V. P. The continued fraction method. Leningrad, 1955.

[3] Müller H. Fractal Scaling Models of Natural Oscillations in Chain Systems and the Mass Distribution of Particles. *Progress in Physics*, 2010, issue 3, 61–66.

[4] Devlin K. The Man of Numbers. Bloomsbury Publ., 2012.

As you can see, only the 10^{th} approximation gives the correct third decimal of ϕ. The approximation process is very slow because of the small denominators. In fact, the denominators in the continued fraction of ϕ are the smallest possible and consequently, the approximation speed is the lowest possible. The golden number ϕ is therefore treated as the "most irrational" number in the sense that a good approximation of ϕ by rational numbers cannot be given with small quotients.

On the contrary, transcendental numbers can be approximated exceptionally well by rational numbers, because their continued fractions contain large denominators and can be truncated with minimum loss of precision. For instance, the simple continued fraction of the circle number $\pi = 3.1415927\ldots = [3;\, 7,\, 15,\, 1,\, 292,\, \ldots]$ delivers the following sequence of rational approximations:

$[3] = 3$
$[3;\, 7] = 3.\overline{142857}$
$[3;\, 7,\, 15] = 3.\overline{14150943396226}$
$[3;\, 7,\, 15,\, 1] = 3.1415929\ldots$

We can see that the 2^{nd} approximation delivers the first 2 decimals correctly, and the 4^{th} approximation shows already 6 correct decimals.

Much like the continued fraction of the golden number ϕ contains only the number 1, a prominent continued fraction[1] of Euler's number contains all natural numbers as denominators and numerators, forming an infinite fractal sequence of harmonic intervals:

$$e = 2 + \cfrac{1}{1 + \cfrac{1}{2 + \cfrac{2}{3 + \cfrac{3}{4 + \cdots}}}}$$

As Euler's number $e = 2.71828\ldots$ is transcendental, it can also be represented as continued fraction with quickly increasing denominators:

$$e = 1 + \cfrac{2}{1 + \cfrac{1}{6 + \cfrac{1}{10 + \cfrac{1}{14 + \cdots}}}}$$

[1] Yiu P. The Elementary Mathematical Works of Leonhard Euler. Florida Atlantic University, 1999, pp. 77–78.

In this way, already the 4^{th} approximation delivers the first 3 decimals correctly and returns in fact the rounded Euler's number $e = 2.71828\ldots$ of 5 decimals' resolution:

$$\begin{array}{l} 1 \\ 3 \\ 2.\overline{714285} \\ 2.7183\ldots \end{array}$$

This special arithmetic property of the continued fractions[1] of transcendental numbers has the consequence that transcendental numbers are distributed near by rational numbers of small quotients.

This can create the impression that complex systems like the solar system provide ratios of physical quantities which correspond with rational numbers. Actually, they correspond with transcendental numbers which are located close to rational numbers.

Only transcendental numbers define the preferred ratios of quantities which avoid destabilizing internal resonance interaction. In this way, they sustain the lasting stability of complex systems. At the same time, a good rational approximation can be induced quickly, if local resonance interaction is required temporarily.

As we have seen, among all transcendental numbers, Euler's number is very special, because its real power function coincides with its own derivatives. Euler's number allows for inhibiting resonance interaction regarding all internal processes and their derivatives.

In the next chapter you will learn that this arithmetic property of Euler's number has the consequence that complex systems tend to establish relations of quantities that coincide with values of the natural exponential function e^x for integer and rational exponents x.

---

[1] Perron O. Die Lehre von den Kettenbrüchen. 1950.

The Fundamental Fractal

There is one fundamental
cause of all effects.

Giordano Bruno

Thanks to Khinchin's discovery, any real number can be represented as a continued fraction. Now let's apply it to the real argument x of the natural exponential function e^x itself:

$$x = [n_0; n_1, n_2, \ldots, n_k]$$

All denominators $n_1, n_2, \ldots, n_k$ of the continued fraction including the free link n_0 are integer (positive and negative whole) numbers. All numerators equal 1. The length of the continued fraction is given by the number k of layers.

The canonical form (all numerators equal 1) does not limitate our conclusions, because every continued fraction with partial numerators different from 1 can be transformed into a canonical continued fraction using the Euler equivalent transformation[1]. With the help of the Lagrange[2] transformation, every continued fraction with integer denominators can be represented as a continued fraction with natural denominators that is always convergent[3].

Now let's look at the fractal distribution of rational eigenvalues of finite continued fractions. The first layer is given by the truncated after n_1 continued fraction:

$$x = [n_0; n_1] = n_0 + \frac{1}{n_1}$$

For the beginning we take $n_0 = 0$. The denominators n_1 follow the sequence of integer numbers ± 1, ± 2, ± 3 etc. The second layer is given

[1] Skorobogatko V. Ya. The Theory of Branched Continued Fractions and mathematical Applications. Moscow, Nauka, 1983.

[2] Lagrange J. L. Additions aux elements d'algebre d'Euler. 1798.

[3] Markov A. A. Selected work on the continued fraction theory and theory of functions which are minimum divergent from zero. Moscow–Leningrad, 1948.

by the truncated after n_2 continued fraction:

$$x = [n_0; n_1, n_2] = n_0 + \cfrac{1}{n_1 + \cfrac{1}{n_2}}$$

Figure 2 shows the first and the second layer in comparison. As you can see, reciprocal whole numbers $\pm 1/2, \pm 1/3, \pm 1/4, \ldots$ are the attractor points of the distribution. In these points, the distribution density always reaches a local maximum. As well, you can recognize that whole numbers $0, \pm 1, \ldots$ are the main attractors of the distribution.

Now let's remember that we are observing the fractal distribution of rational values $x = [n_0; n_1, n_2, \ldots, n_k]$ of the real argument x of the natural exponential function e^x. What we see is the fractal distribution of transcendental numbers of the type e^x on the natural logarithmic scale! And, we can see that near whole number exponents the distribution density of these transcendental numbers is maximum!

Consequently, for integer exponents, the natural exponential function e^x defines attractor points of transcendental numbers and create islands of stability! Let's write them down:

$e^0 = 1$; $e^1 = 2.718\ldots$; $e^2 = 7.389\ldots$; $e^3 = 20.085\ldots$; $e^4 = 54.598\ldots$; $e^5 = 148.413\ldots$; $e^6 = 403.428\ldots$

Figure 2 shows that these islands are not points, but ranges of stability. Integer number exponents like $0, \pm 1, \pm 2, \pm 3, \ldots$ are attractors which form the widest ranges of stability. Half exponents $\pm 1/2$ form smaller islands, one third exponents $\pm 1/3$ form the next smaller islands and one fourth exponents $\pm 1/4$ form even smaller islands of stability.

In this way, the natural exponential function e^x of the rational argument $x = [n_0; n_1, n_2, \ldots, n_k]$ generates the set of preferred ratios of quantities which provide the lasting stability of real processes and structures regardless of their complexity. This is a very powerful conclusion, as we will see in the following.

For rational exponents, the natural exponential function is always transcendental.[1] Increasing the length of the continued fraction, the density of the distribution of transcendental numbers of the type e^x on the natural logarithmic scale is increasing as well. In fact, nearly every irrational number is transcendental, and all irrational numbers together form a continuum.

[1] Hilbert D. Über die Transcendenz der Zahlen e und π. *Mathematische Annalen*, Bd. 43, 216–219, 1893.

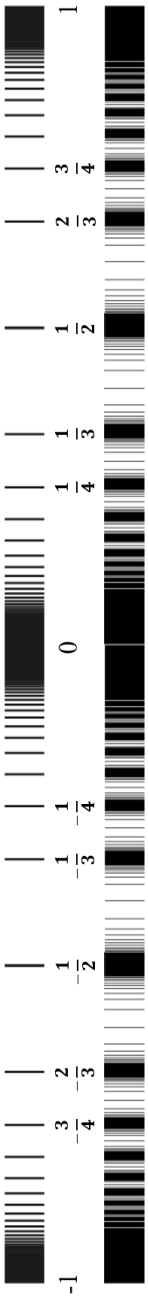

Figure 2: The logarithmic representation of the Fundamental Fractal for $k = 1$ (above) and $k = 2$ (below) in the range $[-1] \ldots [1]$.

Nevertheless, their distribution is not homogeneous, but fractal. Applying continued fractions and truncating them, we can represent the exponents of the natural exponential function e^x as rational numbers and make visible their fractal distribution.

Here I would like to underline that the application of continued fractions doesn't limit the universality of our conclusions, because continued fractions deliver biunique representations of all real numbers including transcendental.

Therefore, the fractal distribution of eigenvalues of the natural exponential function e^x of the real argument x, represented as simple continued fraction, is an inherent characteristic of the number continuum. This characteristic we call the Fundamental Fractal (FF).[1]

Let us remember now that in physical applications, the natural exponential function e^x of the real argument x is the ratio of two physical quantities where one of them is the reference quantity called unit of measurement. Therefore, now we can rewrite our equation:

$$\ln(\mathrm{X}/\mathrm{Y}) = [n_0; n_1, n_2, \ldots, n_k]$$

where X is the measured physical quantity and Y the unit of measurement; ln is the natural logarithm.

Now let's apply this knowledge to our first example of the Venus-to-Earth orbital period ratio 0.61520(2). In this case, X = 0.61520(2) years and Y = 1 year. Let's calculate the natural logarithm of the average: $\ln(0.6152) = -0.49$. We can see that this logarithm is close to $-1/2$. The deviation is only 0.01. Consequently, the Venus-to-Earth orbital period ratio is close to an attractor point of the FF. To reach this attractor point that is the center of a local island of stability, seems that Venus has to increase its orbital velocity slightly.

Indeed, our calculation did not consider all uncertainties in the Venus-to-Earth orbital period ratio. As we have found out, the uncertainty of this ratio appears as consequence of periodic variations in the orbital movement of Venus. Certainly, this is valid not only for Venus, but for all celestial bodies. Also the orbital movement of the Earth is not constant.

---

[1] Müller H. Scale-Invariant Models of Natural Oscillations in Chain Systems and their Cosmological Significance. *Progress in Physics*, issue 4, 187–197, 2017.

The Fundamental Metrology

The Eternal is number, measure,
limit without limit, end without end.

Giordano Bruno

In this context, the question arises whether there is some kind of "absolutely" stable process in the universe?

In fact, such processes do exist. Historically one of them was discovered as cathode rays and named "electron", another as nucleus of the hydrogen atom and named "proton".

The lifespans of the proton and electron[1] surpass everything that is measurable, exceeding 10^{30} years. No scientist ever witnessed the decay of a proton or an electron. Proton and electron form stable atoms, the structural elements of matter.

The exceptional stability and uniqueness of the electron and proton predispose their physical characteristics to be treated as natural and fundamental units of measurement. Table 1 on the next page shows the basic set of electron and proton units (c is the speed of light in a vacuum, $\hbar$ is the Planck constant, k_B is the Boltzmann constant) that we call the Fundamental Metrology.

The Fundamental Metrology is completely compatible with Planck units. Originally proposed in 1899 by Max Planck, they are also known as natural units, because the origin of their definition comes only from properties of nature and not from any human construct. Natural units are based only on the properties of space-time.

Max Planck wrote that these units, "regardless of any particular bodies or substances, retain their importance for all times and for all cultures, including alien and non-human, and can therefore be called natural units of measurement".[2]

Richard Feynman was a student in Princeton in the spring of 1940, when during a telephone conversation, his professor of physics John Wheeler shared with him an idea of cosmological significance. In his speech at the receipt of the Nobel Prize, Feynman recounted this story

[1] Steinberg R. I. et al. Experimental test of charge conservation and the stability of the electron. *Physical Review D.*, 1999, vol. 61 (2), 2582–2586.

[2] Max Planck. Über Irreversible Strahlungsvorgänge. *Sitzungsbericht der Königlich Preußischen Akademie der Wissenschaften*, 1899, vol. 1, 479–480.

PROPERTY	ELECTRON	PROTON
rest mass m	$9.109383 \cdot 10^{-31}$ kg	$1.672622 \cdot 10^{-27}$ kg
energy $\mathrm{E} = \mathrm{m}c^2$	0.5109989 MeV	938.27208 MeV
temperature $\mathrm{T} = \mathrm{E}/k_B$	$5.9298446 \cdot 10^{9}$ K	$1.08881 \cdot 10^{13}$ K
frequency $\omega = \mathrm{E}/\hbar$	$7.763441 \cdot 10^{20}$ Hz	$1.425486 \cdot 10^{24}$ Hz
oscillation period $\tau = 1/\omega$	$1.288089 \cdot 10^{-21}$ s	$7.01515 \cdot 10^{-25}$ s
wavelength $\lambda = c/\omega$	$3.861593 \cdot 10^{-13}$ m	$2.103089 \cdot 10^{-16}$ m
acceleration $a = c\,\omega$	$2.327421 \cdot 10^{29}$ ms^{-2}	$4.2735 \cdot 10^{32}$ ms^{-2}

Table 1: The Fundamental Metrology. Physical characteristics of proton and electron. Data taken from Particle Data Group, www.pdg.lbl.gov

as follows: "Feynman," Wheeler said, "I know why all electrons have the same charge and the same mass." "Why?" Feynman asked. "Because," Wheeler replied, "they are all the same electron!"

In this book we treat the proton and electron as the "metronomes of the universe", as fundamental clocks which are synchronizing the whole universe. Here arises a question: What is the source of their exceptional stability?

In fact, the proton-to-electron ratio 1836.15267389(17) is a fundamental constant[1] and it has the same value for frequencies, oscillation periods, wavelengths, accelerations, energies and masses.

In standard particle physics, the electron is stable because it is the least massive particle with non-zero electric charge. Its decay would violate charge conservation. The proton is stable, because it is the lightest baryon and the baryon number is conserved. Indeed, this answer only readdresses the question. Why then is the proton the lightest baryon? To answer this question, scientists believe in the existence of non-observable entities — the quarks...

Now hold on tight: It may be that the source of the exceptional stability of the proton and electron is the number continuum, more specifically, the proton-to-electron ratio itself is caused by the FF! In fact, the natural logarithm is close to seven and a half:

$$\ln\left(\frac{m_{\,\mathrm{proton}}}{m_{\,\mathrm{electron}}}\right) = \ln\left(1836.15267389\right) \simeq 7 + \frac{1}{2}$$

[1] Physical constants. Particle Data Group. www.pdg.lbl.gov

As a consequence, the proton FF is complementary to the electron FF, because integer logarithms of the proton FF correspond to half logarithms of the electron FF and vice versa, so that the scaling factor $e^{1/2} = \sqrt{e} = 1.64872\ldots$ connects attractor points of proton stability with similar attractor points of electron stability in alternating sequence. Figure 3 on the next page demonstrates this situation.

In the bottom we see the proton FF and in the top the electron FF. Both are represented at the first layer only, so we can see clearly that they have in common only the attractor points $\pm 1/2$, $\pm 1/3$ and $\pm 1/4$. In these attractor points, proton stability is supported by electron stability, so we can expect that they are preferred in complex systems.

By the way, not only the proton-to-electron ratio follows the FF, but also the ratios of other elementary particles do so, even if their lifespans are very short. As table 2 shows, the logarithms of fundamental particle ratios are always close to integer or half values.

PARTICLE	MASS m, MEV/c^2	$\ln(m/m_e)$	FF	$\ln(m/m_e)$–FF
H-boson	125090	12.408	[12;2]	-0.092
Z-boson	91187.6	12.092	[12]	0.092
W-boson	80385	11.966	[12]	-0.034
neutron	939.565379	7.517	[7;2]	0.017
proton	938.27208	7.515	[7;2]	0.015
electron	0.51099894	0.000	[0]	0.000

Table 2: Fundamental particles and the correspondence of their mass ratios with FF-attractors of stability. Data taken from Particle Data Group, www.pdg.lbl.gov

We know already that the islands of stability in the FF are not points but ranges. Integer exponents like 0, ± 1, ± 2, ± 3, ... are attractor points which form the largest islands of stability. Half exponents $\pm 1/2$ form smaller islands, one third exponents $\pm 1/3$ form the next smaller islands and one fourth exponents $\pm 1/4$ form even smaller islands.

Therefore, we can expect that complex systems first occupy the main islands of stability which correspond with integer or half exponents, then the next smaller islands are occupied which correspond with one third exponents and finally those of the one fourth exponents.

Applying this rule to the analysis of measurements we can study the

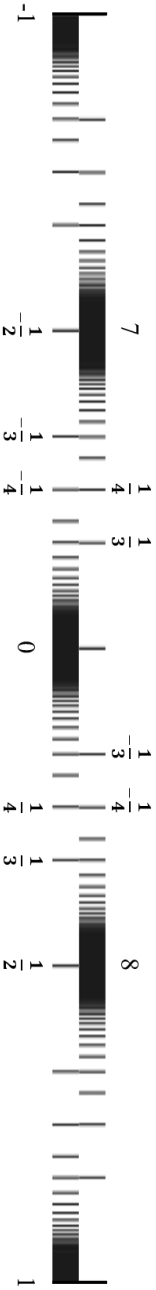

Figure 3: The attractors of both proton (top) and electron (bottom) stability. Natural logarithmic representation.

fractal hierarchy of complex systems and understand their formation.

In astrophysics, it allows for the prediction of orbits of missing celestial bodies in the solar system as well as exoplanets. In biophysics and astrobiology, it allows for studying the interscalar embedding of biological functions in astrophysical processes. In geophysics and planetology, it allows for the prediction of the lithospheric and atmospheric stratification on various planets (see references on pp. 83–84).

Now let's apply the metric characteristics of proton and electron — the Fundamental Metrology — to the analysis of measurements. Let's take our famous example of Venus' orbital period. Let's calculate the natural logarithm of the ratio of Venus' sidereal orbital period to the electron oscillation period:

$$\ln\left(\frac{T_{\text{Venus}}}{2\pi\cdot\tau_{\text{electron}}}\right)=\ln\left(\frac{224.701\cdot 86164\text{ s}}{2\pi\cdot 1.288089\cdot 10^{-21}\text{ s}}\right)=63.04$$

We can see that this logarithm is close to the integer 63. The deviation is only 0.04. Consequently, Venus' orbital period is near the main attractor E[63] of electron stability[1]. This result confirms our early conclusion that Venus has to increase its orbital velocity slightly to reach the attractor point of stability in the FF.

Also the orbital period of the Earth corresponds with a main attractor of stability, but relative to the proton oscillation period:

$$\ln\left(\frac{T_{\text{Earth}}}{2\pi\cdot\tau_{\text{proton}}}\right)=\ln\left(\frac{365.2564\cdot 86164\text{ s}}{2\pi\cdot 7.015150\cdot 10^{-25}\text{ s}}\right)=71.05$$

Probably, also the Earth will increase its orbital velocity slightly. Jupiter's sidereal orbital period[2] coincides perfectly with the main attractor E[66] of electron stability:

$$\ln\left(\frac{T_{\text{Jupiter}}}{2\pi\cdot\tau_{\text{electron}}}\right)=\ln\left(\frac{4332.59\cdot 86164\text{ s}}{2\pi\cdot 1.288089\cdot 10^{-21}\text{ s}}\right)=66.00$$

Jupiter is the largest and heaviest planet in the solar system and fortunately, Jupiter's orbit is perfectly positioned in the FF. Thank God!

Jupiter's rotation period of 9.84 hours coincides with the same main attractor P[66], but of proton stability:

$$\ln\left(\frac{\tau_{\text{Jupiter}}}{\tau_{\text{proton}}}\right)=\ln\left(\frac{9.84\cdot 3600\text{ s}}{7.015150\cdot 10^{-25}\text{ s}}\right)=66.09$$

[1] Here and in the following we use the letter E for electron stability and the letter P for proton stability.

[2] Jupiter Fact Sheet. NASA Space Science Archive. www.nssdc.gsfc.nasa.gov

When the sidereal rotation period of Jupiter slows down to P[66] = 9 hours, the orbital-to-rotation period ratio of Jupiter can be described by the equation:

$$\frac{T_{\,\mathrm{Jupiter}}}{\tau_{\mathrm{Jupiter}}} = 2\pi \frac{\tau_{\,\mathrm{electron}}}{\tau_{\mathrm{proton}}}$$

By the way, the rotation period 9.074 hours of the planetoid Ceres fits perfectly with the same attractor P[66].

Although the rotation of Venus is reverse, its rotation period of 5816.66728 hours fits with the main attractor E[65]:

$$\ln\left(\frac{\tau_{\,\mathrm{Venus}}}{\tau_{\mathrm{electron}}}\right) = \ln\left(\frac{5816.66728 \cdot 3600\ \mathrm{s}}{1.288089 \cdot 10^{-21}\ \mathrm{s}}\right) = 64.96$$

The sidereal rotation period of Mars is 24.62278 hours and coincides perfectly with the main attractor P[67]:

$$\ln\left(\frac{\tau_{\,\mathrm{Mars}}}{\tau_{\mathrm{proton}}}\right) = \ln\left(\frac{24.62278 \cdot 3600\ \mathrm{s}}{7.015150 \cdot 10^{-25}\ \mathrm{s}}\right) = 67.01$$

Naturally, Earth's rotation period 23.93444 hours coincides with the same attractor P[67]. The sidereal rotation period of Mercury is 1407.5 hours and coincides with the main attractor P[71]:

$$\ln\left(\frac{\tau_{\,\mathrm{Mercury}}}{\tau_{\mathrm{proton}}}\right) = \ln\left(\frac{1407.5 \cdot 3600\ \mathrm{s}}{7.01515 \cdot 10^{-25}\ \mathrm{s}}\right) = 71.05$$

The sidereal rotation period of Neptune is 16.11 hours and coincides with the main attractor E[59]:

$$\ln\left(\frac{\tau_{\,\mathrm{Neptune}}}{\tau_{\mathrm{electron}}}\right) = \ln\left(\frac{16.11 \cdot 3600\ \mathrm{s}}{1.288089 \cdot 10^{-21}\ \mathrm{s}}\right) = 59.07$$

The rotation periods[1] of Saturn (10.55 h), Uranus (17.24 h) and Pluto (152.875 h) coincide with the sub-attractors E[59;−3], P[67;−3], E[61;3] respectively.

Figure 4 shows how the orbital periods of planets and planetoids of the solar system are distributed in the FF. We can see that the majority of planets has occupied main attractors of electron stability.

The Earth is the only planet that occupies a main attractor of proton stability. Mercury, Mars, Eris and Neptune occupy sub-attractors of the same type $[n_0; \pm 3]$.

[1] NASA Space Science Coordinated Archive. www.nssdc.gsfc.nasa.gov

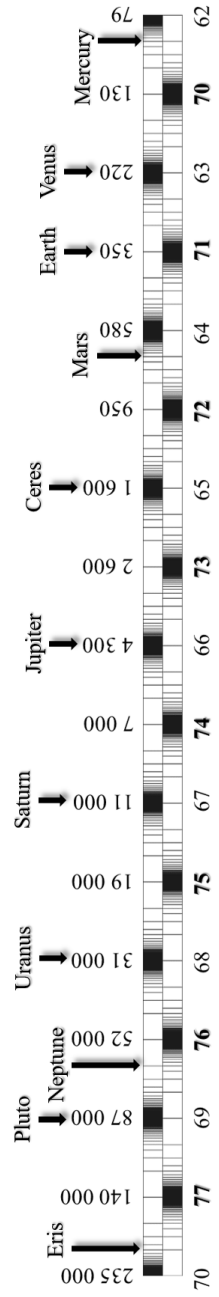

Figure 4: The correspondence of the sidereal orbital periods of planets and planetoids with attractors of proton (lower FF) and electron (upper FF) stability. Orbital periods (top) in days.

Not only the solar system, but also exoplanetary systems like Trappist[1] or Kepler[2] follow the FF. Also exoplanetary orbits are positioned close to attractor points of proton or electron stability.

It is remarkable that the orbits of Trappist 1b, c, d and e correspond with main attractors. This is also valid for Kepler 20b, d and e and for many other exoplanetary systems we do not discuss in this book. Therefore, their orbital periods can coincide with those in the solar system. For example, planets in the Trappist 1 system have the same orbital periods as have the moons of Jupiter, Saturn, Uranus and Neptune, as shows figure 5.

The origin of the FF is the number continuum. Consequently, not only planetary systems follow the FF, but everything in the universe does so. Naturally, biological processes are not an exception. For instance, the average adult human relaxed heart rate[3] of 60–70 beats per minute is close to the main attractor E[−48] of electron stability:

$$\ln\left(\frac{\omega_{\,\text{heart}}}{\omega_{\,\text{electron}}}\right) = \ln\left(\frac{66/60\ \text{Hz}}{7.763441\cdot 10^{20}\ \text{Hz}}\right) = -48$$

The average adult human relaxed breathing[4] rate of 13–17 breaths per minute is close to the main attractor P[−57] of proton stability:

$$\ln\left(\frac{\omega_{\,\text{breathing}}}{\omega_{\,\text{proton}}}\right) = \ln\left(\frac{15/60\ \text{Hz}}{1.425486\cdot 10^{24}\ \text{Hz}}\right) = -57$$

The EEG frequency ranges[5] of Theta (3–7 Hz), Alpha (8–13 Hz) and Beta (14–33 Hz) brain activity follow precisely the FF:

The lower Theta limit of 3 Hz coincides with the main attractor E[−47], the Theta-Alpha boundary of 7–8 Hz coincides with E[−46], the Alpha-Beta boundary of 13–14 Hz coincides with P[−53] and the upper Beta limit of 33 Hz fits perfectly with the main attractor P[−52] of proton stability.

---

[1] Gillon M. et al. Seven temperate terrestrial planets around the nearby ultracool dwarf star TRAPPIST-1. *Nature*, vol. 542(7642), 456–460, 2017.

[2] Hand E. KEPLER discovers first Earth-sized exoplanets. *Nature.com*, 20 Dec. 2011.

[3] Spodick D. H. Survey of selected cardiologists for an operational definition of normal sinus heart rate. *The American J. of Cardiology*, 1993, vol. 72 (5), 487–488.

[4] Ganong's Review of Medical Physiology (23rd ed.), p. 600.

[5] Tesche C. D., Karhu J. Theta oscillations index human hippocampal activation during a working memory task. *PNAS*, vol. 97, no. 2, 2000.

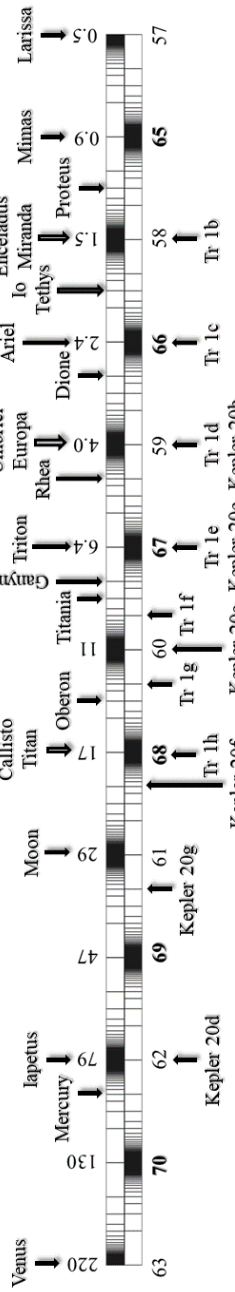

Figure 5: The correspondence of sidereal orbital periods with attractors of proton (lower FF) and electron (upper FF) stability for large moons of Jupiter, Saturn, Uranus, Neptune and exoplanets of Trappist 1 and Kepler 20. Orbital periods (top) in days.

The Fundamental Field

There is in the universe
neither center
nor circumference.

Giordano Bruno

Until now we did apply the FF to the analysis of frequencies and oscillation periods. Now let's calibrate the FF on the proton and electron wavelengths and apply the spatial projection of the FF to the analysis of sizes and distances.

The number of layers of the FF is not limited. Therefore, in each point of the space-time a scalar (real number) is defined — the eigenvalue of the FF. In this way, the FF creates a fractal scalar field, the Fundamental Field.[1]

Figure 6 shows the linear spatial 2D-projection of the first layer of the Fundamental Field e^x for $x = n_0 + 1/n_1$ in the interval $-1 < x < 1$. Figure 2 on page 17 shows the same interval in the logarithmic representation. Figure 7 shows the linear 2D-projection of the FF with both proton and electron attractors of stability.

The Fundamental Field is the spatio-temporal projection of the Fundamental Fractal. For both we use the abbreviation FF. The connection between the spatial and temporal projections of the FF is given by the speed of light in a vacuum $c = 299792458$ m/s. The constancy of c makes both projections isomorphic, so that there is no arithmetic or geometric difference. Only the units of measurement are different.

Figures 6 and 7 show the spatial 2D-projection, but in reality the FF is 3-dimensional, a sphere with fractal layers inside like an onion.

At each layer, the potential energy of the Fundamental Field is constant, therefore the layers are called equipotential surfaces. The potential difference defines a gradient, a vector directed to the center of the field that causes a central force of attraction. Indeed, the Fundamental Field is fractal so that the gradient isn't always directed to the center, but exposes the internal fractality of the FF.

[1] Müller H. Quantum Gravity Aspects of Global Scaling and the Seismic Profile of the Earth. *Progress in Physics*, issue 1, 41–45, 2018.

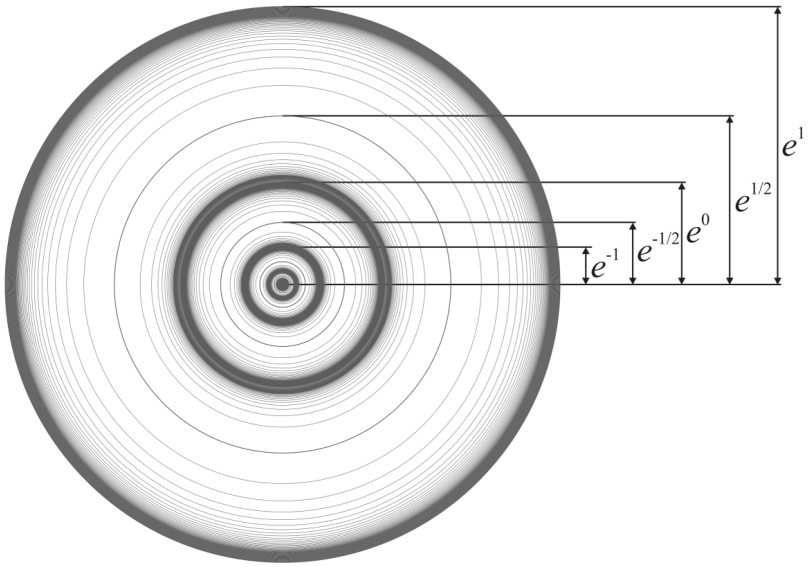

Figure 6: The equipotential surfaces of the Fundamental Field in the linear 2D-projection for $k = 1$.

Considering its arithmetic origin, we postulate that all types of physical interaction including the electromagnetic, nuclear and gravitational, originate from the FF. In view of this, they differ only in scale.

What about the field source, the electrical charge, for instance? The appearance of a field source is only an effect of linear observation. You can recognize this effect in figure 6. Whereas the logarithmic pattern of the FF is the same in all scales, its linear density increases exponentially in the direction of smaller scales, creating the effect of an existing field source. In contrast, in the direction of larger scales, the linear density is decreasing, creating the effect of an accelerating expansion of the FF.

Reading this, aren't you reminded of something? Right, we are reminded of the Big Bang model of an expanding universe! We realize that the expansion of the universe is only an effect of linear observation that is difficult to explain if you don't know the FF.

Consequently, in the solar system, in the Galaxy or in any other complex system where internal resonance interaction has to be avoided for reasons of stability, the involved physical fields should expose the inherent structure of the FF. In fact, analyzing distances in the solar

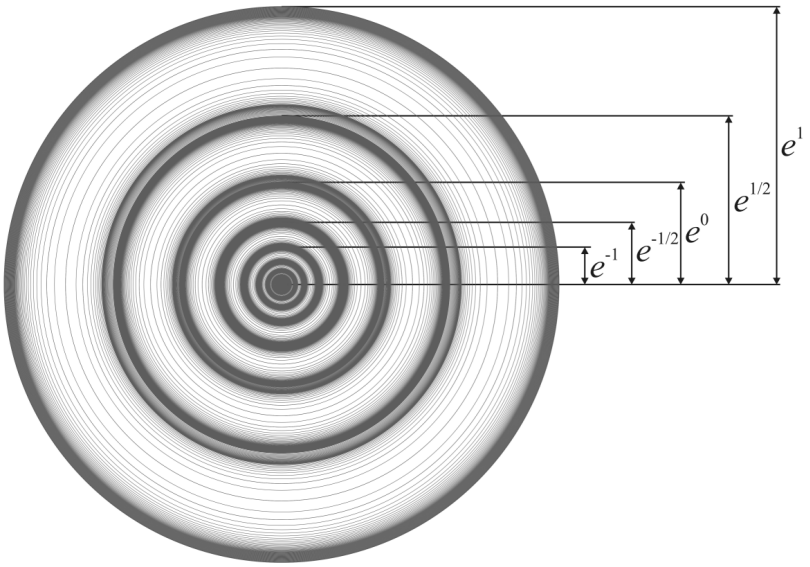

Figure 7: The Fundamental Field with equipotential surfaces of both proton and electron attractors of stability in the linear 2D-projection for $k = 1$.

system, we can see that the orbits of planets and moons coincide with equipotential surfaces of the FF, because movement along an equipotential surface requires no work.

For example, the orbital distance[1] of Venus coincides with the main equipotential surface E[54] of electron stability:

$$\ln\left(\frac{R_{\,\mathrm{Venus}}}{\lambda_{\,\mathrm{electron}}}\right) = \ln\left(\frac{1.08939 \cdot 10^{11}\ \mathrm{m}}{3.861593 \cdot 10^{-13}\ \mathrm{m}}\right) = 54$$

where $R_{\,\mathrm{Venus}} = 0.723332\,\mathrm{AU} = 1.08939 \cdot 10^{11}$ m is the semi-major axis of Venus' orbit, $\lambda_{\,\mathrm{electron}} = 3.861593 \cdot 10^{-13}$ m is the Compton wavelength of the electron (see table 1 on page 20). Earth's orbital distance coincides with the equipotential surface E[54;3]:

$$\ln\left(\frac{R_{\,\mathrm{Earth}}}{\lambda_{\,\mathrm{electron}}}\right) = \ln\left(\frac{1.49598023 \cdot 10^{11}\ \mathrm{m}}{3.861593 \cdot 10^{-13}\ \mathrm{m}}\right) = 54 + \frac{1}{3}$$

The mean orbital distance of Jupiter coincides with the main equipo-

[1] Venus Fact Sheet. NASA Space Science Archive. www.nssdc.gsfc.nasa.gov

tential surface E[56] of electron stability:

$$\ln\left(\frac{R_{\,\text{Jupiter}}}{\lambda_{\,\text{electron}}}\right)=\ln\left(\frac{7.7857\cdot10^{11}\ \text{m}}{3.861593\cdot10^{-13}\ \text{m}}\right)=56$$

Now you can understand that the knowledge of the FF opens the possibility to develop a completely new vision of the solar system. The origin of this vision is the number continuum and therefore, it is not only precise, but universal and applicable to all systems in the Galaxy.

The spatial projection of the FF determines not only the orbital systems, but also the sizes of stars, planets and moons. For example, the radius of Sirius A photosphere[1] coincides with the main equipotential surface P[57] of proton stability:

$$\ln\left(\frac{r_{\,\text{Sirius}}}{\lambda_{\,\text{proton}}}\right)=\ln\left(\frac{1.19155\cdot10^{9}\ \text{m}}{2.103089\cdot10^{-16}\ \text{m}}\right)=57$$

The radius of the Sun's photosphere coincides with the main equipotential surface E[49] of electron stability:

$$\ln\left(\frac{r_{\,\text{Sun}}}{\lambda_{\,\text{electron}}}\right)=\ln\left(\frac{6.96407\cdot10^{8}\ \text{m}}{3.861593\cdot10^{-13}\ \text{m}}\right)=49$$

The radius of the photosphere is considered as the Sun's "surface" in the definition of the surface gravity acceleration of the the Sun[2] that is actually 274 m/s^2, it is 28 times stronger than gravity on the Earth's surface. Sun's surface gravity coincides with the main attractor E[−62]:

$$\ln\left(\frac{g_{\,\text{Sun}}}{a_{\,\text{electron}}}\right)=\ln\left(\frac{274\ \text{m/s}^2}{2.327421\cdot10^{29}\,\text{m/s}^2}\right)=-62$$

All units of measurement we are using are taken from the Fundamental Metrology, see table 1 on page 20. Jupiter's surface gravity coincides with the main attractor P[−72] of proton stability:

$$\ln\left(\frac{g_{\,\text{Jupiter}}}{a_{\,\text{proton}}}\right)=\ln\left(\frac{24.8\ \text{m/s}^2}{4.273500\cdot10^{32}\,\text{m/s}^2}\right)=-72$$

[1] Liebert J. et al. The Age and Progenitor Mass of Sirius B. *The Astrophysical Journal*, vol. 630 (1), 69–72. arXiv:astro-ph/0507523.

[2] Sun Fact Sheet. NASA Space Science Archive. www.nssdc.gsfc.nasa.gov

Venus and Uranus have the same surface gravity that coincides with the main attractor P[−73] of proton stability:

$$\ln\left(\frac{g_{\,\text{Venus}}}{a_{\,\text{proton}}}\right) = \ln\left(\frac{8.8\ \text{m/s}^2}{4.273500\cdot 10^{32}\,\text{m/s}^2}\right) = -73$$

Mars and Mercury have the same surface gravity that coincides with the sub-attractor E[−66;−3] of electron stability:

$$\ln\left(\frac{g_{\,\text{Mars}}}{a_{\,\text{electron}}}\right) = \ln\left(\frac{3.7\ \text{m/s}^2}{2.327421\cdot 10^{29}\,\text{m/s}^2}\right) = -66-\frac{1}{3}$$

Earth's surface gravity coincides with the sub-attractor E[−65;−3]:

$$\ln\left(\frac{g_{\,\text{Earth}}}{a_{\,\text{electron}}}\right) = \ln\left(\frac{9.8\ \text{m/s}^2}{2.327421\cdot 10^{29}\,\text{m/s}^2}\right) = -65-\frac{1}{3}$$

It is always the same logic: If it is vital for the system that some ratio of quantities remains stable, for example the orbital period of Jupiter in relation to the oscillation periods of proton and electron, then this ratio should be as close as possible to an FF-attractor point of stability.

Having this position in the FF, the ratio of quantities doesn't have to fit precisely with an attractor point, because near an attractor point this ratio is "swimming" in a pool of transcendental numbers.

Here I want to underline that the Fundamental Field does not propagate, it is omnipresent. The Fundamental Field is the spatio-temporal projection of the Fundamental Fractal that is an inherent feature of the number continuum. The FF causes the fractality of space-time.

In physics, only field distortions (waves or currents), not the fields themselves have propagation speeds. In astronomic calculations, gravitation is traditionally considered as being instantaneous. First Laplace[1] demonstrated that gravitation as field does not propagate with the speed of light c. Modern estimations[2] confirm a lower limit of $2\cdot 10^{10}\,c$.

Also, the quantization of orbital systems is not a random solution. The solution is given a priori and it is omnipresent. Therefore, we find that orbital quantization follows the FF also in exoplanetary systems (see figure 5 on page 27).

---

[1] Laplace P. Mechanique Celeste. 1825, pp. 642–645.

[2] Van Flandern T. The Speed of Gravity — What the Experiments Say. *Physics Letters A*, vol. 250, 1–11, 1998.

Global Scaling

> Anything we take in the universe
> has in itself that which is All in All.
>
> *Giordano Bruno*

The Fundamental Fractal is of pure mathematical origin, and there is no particular physical mechanism required as creator of the Fundamental Field. It is all about numbers as ratios of physical quantities which can provoke destabilizing resonance or inhibit it. In this way, the FF concerns all repetitive processes which share at least one characteristic — the frequency.

A general resonance condition is given by rational frequency ratios. This condition does not compellingly cause resonance, but increases dramatically the probability of its occurrence. Primarily, the FF defines the distribution of those frequency ratios that inhibit resonance.

In the case of quantum oscillators, the FF defines also the ratios of wavelengths, velocities, energies, masses and other physical quantities which inhibit resonance and in this way, support lasting stability. It is because many physical characteristics of quantum oscillators are connected with their frequency by fundamental constants — the speed of light in a vacuum and the Planck constant.

Within the ocean of quantum oscillators in the universe, there are only two of exceptional stability — electron and proton. They form atoms — the stable elements of the universe. You remember that the proton-to-electron ratio satisfies the condition of main attractors of stability in the FF. This is why the FF affects everything in the universe and is of cosmological significance. Probably, the FF is some kind of "matrix of the universe".

Indeed, the electron and the proton are not the ultimate sources, but stability nodes of the FF. The spatial and temporal distribution of these stability nodes is determined by Euler's number. Already Paul Dirac[1] mentioned that "... whether a thing is constant or not does not have any absolute meaning unless that quantity is dimensionless".

By the way, in German, "knowing from the FF" means that you know something by heart and you can do it "on the fly", because you

[1] Dirac P. A. M. The cosmological constants. *Nature*, vol. 139, 1937.

got not only a single aspect, but also all the following pages of the topic. The term comes from Latin "ex forma, ex functione". In Italy, "ff" has various historical meanings: "fiat fiat" (imperative order), "fortissimo" (powerful) and "finissimo" (very thin). I think that even these sayings describe some features of our FF.

Now I would like to guide your attention to a very important feature of the FF. As you already know, in the logarithmic representation, the main attractors show an equidistant distribution (see figure 4 on page 25). Neighboring main attractors of the same calibration (E or P) are always separated by one unit of the natural logarithm. Consequently, if one main attractor is known, all the others can be calculated simply by multiplication with Euler's number. This feature of the FF is called "scale invariance" or "scaling".

Consequently, it is sufficient to know one metric characteristic of the electron or proton to calculate the complete FF in all scales of the universe with all attractors and sub-attractors of electron or proton stability. This feature we call "Global Scaling".[1]

Already in 1795, Karl Friedrich Gauss discovered scaling in the distribution of prime numbers. As natural phenomenon, scaling was discovered probably first in biophysics by Gustav Fechner[2] and Ernst Weber. Then in seismology, Beno Gutenberg and Charles Richter[3] have shown that there exists a logarithmic invariant (scaling) relationship between the energy (magnitude) and the total number of earthquakes in a given region and time period.

In the sixties, Richard Feynman and James Bjorken[4] discovered scaling in particle physics. In the eighties, the scaling exponent 3/2 was found in the distribution of particle masses by Valery A. Kolombet.[5] In the last 40 years many studies were published which show that scaling is a widely distributed phenomenon.[6]

Reading this book, you will learn that Global Scaling is a universal characteristic of organized matter and criterion of stability. As we have already seen, Global Scaling is a forming factor of the solar system.

---

[1] Müller H. Scale-Invariant Models of Natural Oscillations in Chain Systems and their Cosmological Significance. *Progress in Physics*, issue 4, 187–197, 2017.

[2] Fechner G. T. Elemente der Psychophysik, Bd. 2, 1860.

[3] Gutenberg B., Richter C. F. Seismicity of the Earth and associated phenomena. Princeton University Press, 1954.

[4] Feynman R. P. Very high-energy collisions of hadrons. *Phys. Rev. Lett.*, vol. 23, 1415, 1969; Bjorken J. D. *Phys. Rev. D*, vol. 179, 1547, 1969.

[5] Kolombet V. Macroscopic fluctuations, masses of particles and discrete space-time. *Biofizika*, 1992, vol. 36, 492–499.

[6] Barenblatt G. I. Scaling. Cambridge University Press, 2003.

In this book you will learn that Global Scaling forms also the fractal structure of the Earth's interior and of planetary atmospheres.

The FF defines the fractal hierarchy of attractors which are islands of stability in very different scales — from the subatomic to the galactic. Now let's come back to the first question I asked at the beginning of this book. Why is the universe so large and at the same time so small? Naturally, you already know the answer: It is because of the logarithmic scale invariance of the FF. Let us take an example. Hydrogen (protium) is the smallest atom and its atomic radius 22 pm coincides with the main attractor E[4] of electron stability:

$$\ln\left(\frac{r_{\,\mathrm{hydrogen}}}{\lambda_{\,\mathrm{electron}}}\right) = \ln\left(\frac{2.2\cdot 10^{-11}\ \mathrm{m}}{3.861593\cdot 10^{-13}\ \mathrm{m}}\right) = 4$$

Adding 12 units of the natural logarithm we find the attractor E[16] = 3.4 μm that is occupied by the smallest living cell, the mycoplasma:

$$\ln\left(\frac{r_{\,\mathrm{mycoplasma}}}{\lambda_{\,\mathrm{electron}}}\right) = \ln\left(\frac{3.4\cdot 10^{-6}\ \mathrm{m}}{3.861593\cdot 10^{-13}\ \mathrm{m}}\right) = 16$$

Adding another 12 logarithmic units we find the attractor E[28] = 55 cm, the body length of a newborn.

The same scale-difference of 12 natural logarithmic units divides the scale of the Galaxy P[84] and the scale of the solar system P[72] that appears in the Galaxy like an atom in a living cell. On the logarithmic scale it is always the same distance, but in linear space-time it can be subatomic or interstellar.

The FF neither expands nor condenses into a point. The FF is of arithmetical origin and so, it is an eternal constant that forms the universe in all scales. Global Scaling is the conceptual basis of interscalar cosmology.

Whereas standard cosmology[1] studies the large-scale structures and dynamics in the universe to understand its origin, evolution and "ultimate fate", the basis of interscalar cosmology is the study of the universe in all scales, considering the FF as universal matrix of stability.

Interscalar cosmology considers that the apparent dominance of large scale dynamics in the universe is only a scaling-effect of observation.

Established systems like atoms, living cells, organisms, planetary systems or galaxies are always realizations of the same matrix — the FF. In the universe there are no more or less important scales.

[1] Ellis G. Issues in Philosophy of Cosmology. arXiv:astro-ph/0602280v2, 2006.

That's why it is difficult to understand the nature of the universe considering only large scales. Naturally, such cosmological models can't be considered as complete and their affirmations about the origin, evolution and "ultimate fate" of the universe should be perceived with healthy scepticism. Let's see together a prominent example.

Observing the sky with a traditional optical telescope, the space between stars and galaxies only seems completely dark. Actually, sensitive radio telescopes receive a faint background noise, or glow, that is not associated with any star, galaxy, or other object.

This glow is strongest in the microwave region of the radio spectrum. Accidentally discovered in 1964 by the American radio astronomers Arno Penzias and Robert Wilson, it was named cosmic microwave background radiation (CMBR).

In Big Bang cosmology, the CMBR is interpreted as a remnant from an early stage of the observable universe. According to this theory, when the universe was young, stars and planets didn't exist yet, and it was denser, much hotter, and filled with a uniform glow from a hot fog of hydrogen plasma. As the universe expanded, both the plasma and the radiation filling it grew cooler.

Admittedly, there are alternative models[1] in development proposing explanations for the CMBR which do not implicate standard cosmological scenarios. However, traditionally CMBR data is considered as critical to cosmology since any proposed model of the universe must explain this radiation.

Within Global Scaling, there is no need for a hot prehistory of the universe, no need for any Big Bang and no need for after-cooling. In short, the CMBR is nothing special or out of the ordinary. It is of the same subatomic origin as any electromagnetic radiation in the universe.

If this process is stable, it should correspond with an attractor of the FF. In fact, the average temperature 2.725 Kelvin of the CMBR[2] corresponds to the main attractor P[−29] of proton stability:

$$\ln\left(\frac{\mathrm{T}_{\,\mathrm{CMBR}}}{\mathrm{T}_{\,\mathrm{proton}}}\right) = \ln\left(\frac{2.725\ \mathrm{K}}{1.08881 \cdot 10^{13}\ \mathrm{K}}\right) = -29.015$$

and coincides perfectly with the attractor E[−21;−2] of electron stabil-

[1] Lopez-Corredoira M. Non-standard models and the sociology of cosmology. Science Direct, *Studies in History and Philosophy of Modern Physics*, vol. 46, Part A, May 2014, pp. 86–96.

[2] Fixsen D. J. The Temperature of the Cosmic Microwave Background. *The Astrophysical Journal*, vol. 707 (2), 916–920. arXiv:0911.1955, 2009.

ity:

$$\ln\left(\frac{\mathrm{T}_{\,\mathrm{CMBR}}}{\mathrm{T}_{\,\mathrm{electron}}}\right) = \ln\left(\frac{2.725\ \mathrm{K}}{5.9298446 \cdot 10^{9}\ \mathrm{K}}\right) = -21.50$$

By the way, the average temperature 5000 K of the Sun[1] (corona) coincides with the same attractor P[−21;−2], but of proton stability:

$$\ln\left(\frac{\mathrm{T}_{\,\mathrm{Sun}}}{\mathrm{T}_{\,\mathrm{proton}}}\right) = \ln\left(\frac{5000\ \mathrm{K}}{1.08881 \cdot 10^{13}\ \mathrm{K}}\right) = -21.50$$

In this way, Global Scaling analysis shows that both processes are interconnected. This connection could indicate that the CMBR and the solar radiation are of the same origin. Actually, the Planck satellite, even though orbiting the Earth outside the atmosphere, is still deeply inside the heliosphere. In fact, global asymmetry in the CMBR has been reported[2] that is aligned with the plane of the solar system.

Knowing the FF, it is clear that there is no isotropic process in the universe, and it isn't surprising that this is valid also for the CMBR. Increasingly precise data provided by the WMAP and Planck missions made this anisotropy visible.

In contrast to conventional cosmology, interscalar cosmology is not based on the study of the universe only in largest scales. On the contrary, Global Scaling concerns the stability of any process in any scale of the universe.

The FF defines the ratios of quantities which preserve processes and structures from destructive internal resonance. As you already know, within Global Scaling, resonance conditions can be expressed in terms of frequency ratios or ratios of any other metric process characteristics, because Global Scaling deals with stable quantum oscillators — the proton and electron.

In quantum physics, the Boltzmann constant converts energy ratios into ratios of temperatures (see table 1 on page 20). In this case, frequency ratios can be also expressed as ratios of temperatures, naturally only if there is no significant dependency on other thermodynamic parameters.

Fortunately, the melting points of several substances do not show strong dependency on pressure and other environmental conditions. For pure chemical elements, the melting point is identical to the freezing point and remains constant throughout the melting process. Therefore,

[1] Sun Fact Sheet. NASA Space Science Archive. www.nssdc.gsfc.nasa.gov

[2] Santos L. Influence of Planck foreground masks in the large angular scale quadrant CMB asymmetry. arXiv:1510.01009v1, 2015.

we can expect that the melting points of pure chemical elements correspond with attractors of proton or electron stability. You remember that attractor points are points of change, where compression switches to decompression and vice versa. This change can cause the transition from solid to liquid state, for example.

In fact, the melting[1] point 0.955 K of helium 4 (under high pressure) coincides with the main attractor P[−30]:

$$\ln\left(\frac{\mathrm{T}_{\mathrm{He}}}{\mathrm{T}_{\mathrm{proton}}}\right) = \ln\left(\frac{0.955\ \mathrm{K}}{1.08881 \cdot 10^{13}\ \mathrm{K}}\right) = -30$$

The melting point 14 K of hydrogen (protium) coincides with the main attractor E[−20], the melting points 19 K of deuterium and 20 K of tritium coincide with the main attractor P[−27] and the melting point 55 K of oxygen 16 coincides with the main attractor P[−26].

In this way, we can see that the melting points of the elements of highest abundance in the solar system and the Galaxy (H, ^{4}He, ^{16}O) coincide with main attractors of stability.

Now you can comprehend that the correspondence of the average temperature of the CMBR with the main attractor P[−29] cannot astonish anybody who is familiar with the FF. Within Global Scaling, the CMBR represents not more and not less than a stable energy level of the omnipresent protons and electrons. For lack of empirical confirmation, the Big Bang cosmology overrates the CMBR dramatically.

Actually, any process that corresponds with attractors of proton and electron stability is of cosmological significance, because it forms that universe we experience every day. Every atom is a universe, every living cell is a universe, every animal and each of us is a universe, the Earth is a universe, the solar system is a universe and the Milky Way is a universe. All the galaxies together form the universe of the universes that follows the same Global Scaling law of the number continuum as do all the other embedded universes.

---

[1] Periodic table of elements. Los Alamos National Lab., www.periodic.lanl.gov

Interscalar Cosmology

> The countless worlds in the universe
> are no worse and no less inhabited
> than our Earth.
>
> *Giordano Bruno*

Perhaps you are starting to understand that the abundance of coincidences we mentioned in the introduction of this book is caused by the FF of space-time that leads to interscalar cosmology, a completely new understanding of the universe.

Let's take some more examples. Saturn's body radius[1] coincides with the main equipotential surface P[54] of proton stability:

$$\ln\left(\frac{r_{\,\text{Saturn}}}{\lambda_{\,\text{proton}}}\right) = \ln\left(\frac{6.0268 \cdot 10^{7}\ \text{m}}{2.103089 \cdot 10^{-16}\ \text{m}}\right) = 54$$

The main Theta-wave frequency 5 Hz of brain activity has the same wavelength and coincides with the same attractor P[−54]:

$$\ln\left(\frac{\omega_{\,\text{theta}}}{\omega_{\,\text{proton}}}\right) = \ln\left(\frac{5\ \text{Hz}}{1.425486 \cdot 10^{24}\ \text{Hz}}\right) = -54$$

In this way, the FF creates an abundance of interscalar connections. The FF connects not only biological frequencies, but also other biophysical characteristics with astrophysical processes. For example, the average adult human brain[2] mass 1.4 kg corresponds with the main attractor P[62] of proton stability ($1.6726219 \cdot 10^{-27}$ kg is the proton rest mass):

$$\ln\left(\frac{m_{\,\text{human brain}}}{m_{\,\text{proton}}}\right) = \ln\left(\frac{1.4\ \text{kg}}{1.672622 \cdot 10^{-27}\ \text{kg}}\right) = 62$$

The proton attractor P[62] coincides with the electron attractor E[69;2], because $69\ \frac{1}{2} = 62 + 7\ \frac{1}{2}$. Amazingly, the doubled logarithm $69\ \frac{1}{2} + 69\ \frac{1}{2} = 139$ returns the attractor of electron stability E[139] that is occupied by the body mass of the Sun:

$$\ln\left(\frac{M_{\,\text{Sun}}}{m_{\,\text{electron}}}\right) = \ln\left(\frac{1.98855 \cdot 10^{30}\ \text{kg}}{9.109383 \cdot 10^{-31}\ \text{kg}}\right) = 139$$

[1] Saturn Fact Sheet. NASA Space Science Archive. www.nssdc.gsfc.nasa.gov

[2] Singh D. et al. Weights of human organs at autopsy. *JIAFM*, vol. 26 (3), 2004.

Therefore, we can write down the equation:

$$\ln\left(\frac{M_{\,\mathrm{Sun}}}{m_{\,\mathrm{electron}}}\right) = 2\,\ln\left(\frac{m_{\,\mathrm{human\,brain}}}{m_{\,\mathrm{electron}}}\right)$$

Applying the FF, we discovered that the mass of the Sun as well as the average human brain mass correspond with main attractors of stability which have an interscalar connection given by the ratio of their logarithms.

In mathematics, the ratio of logarithms is called fractal dimension of similarity. First introduced in 1919 by Hausdorff[1], it is a standard measure of fractality of both structures and processes.

Before going ahead with mathematics, I would like to mention one more interscalar connection: Whereas the human brain mass corresponds with the attractor P[62] of proton stability, the Sun's surface gravity (p. 31) corresponds with the same main attractor E[62], but of electron stability! Therefore, we can write the equation:

$$\frac{m_{\,\mathrm{brain}}}{m_{\,\mathrm{proton}}} = \frac{a_{\,\mathrm{electron}}}{g_{\,\mathrm{Sun}}}$$

In this equation, $m_{\,\mathrm{brain}} = 1.4$ kg is the average adult human brain mass, $m_{\,\mathrm{proton}} = 1.672622 \cdot 10^{-27}$ kg is the proton rest mass, $a_{\,\mathrm{electron}} = 2.327421 \cdot 10^{29}\,\mathrm{m/s^2}$ is the electron angular acceleration, $g_{\,\mathrm{Sun}} = 274\,\mathrm{m/s^2}$ is the Sun's gravity acceleration (at the photosphere). Rewriting this equation, we get two equal forces:

$$m_{\,\mathrm{brain}} \cdot g_{\,\mathrm{Sun}} = m_{\,\mathrm{proton}} \cdot a_{\,\mathrm{electron}}$$

By the way, in this equation proton and electron can be interchanged:

$$m_{\,\mathrm{electron}} \cdot a_{\,\mathrm{proton}} = m_{\,\mathrm{proton}} \cdot a_{\,\mathrm{electron}} = 389.2895\,N$$

So we have got an astonishing result: the human brain in the gravity field of the Sun weighs exactly the same as the electron weighs in the acceleration field of the proton!

All by chance? I don't think so. First, the human brain mass corresponds with a main attractor of proton stability. Second, the Sun's gravity acceleration corresponds with the same attractor of electron stability. Third, the rest masses of proton and electron are fundamental constants.

[1] Hausdorff F. Dimension und äußeres Maß. *Mathematische Annalen*, vol. 122, issue 1–2, 157–179, 1919.

What could be the meaning of this remarkable coincidence? I would like to propose an astrobiological[1] interpretation. Obviously, biological organisms are part of the solar system and consequently, their physical characteristics are embedded in the system.

Let's see some more examples. As you already know, the Sun's radius coincides with the main equipotential surface E[49] of electron stability. Dividing by 2 gives us the logarithm $49/2 = 24\ \frac{1}{2}$ of the wavelength $\lambda_{\,\text{electron}} \cdot \exp(24.5) = 16.6$ mm that coincides with the focal length of the human eye that is also the length of the newborn eyeball.

As you know, the radius of Saturn coincides with the main equipotential surface P[54] of proton stability. Dividing by 2 we receive the logarithm $27 = 54/2$ of the wavelength $\lambda_{\,\text{proton}} \cdot \exp(27) = 0.11$ mm that coincides with the size of the human fertile oocyte, the zygote.

Probably, biological organisms on exoplanets are also embedded in their systems and therefore we can expect that the physical characteristics of their physiology correspond with the physical characteristics of their sun and planets.

To continue this topic let us look at our own organism through the FF. We begin with the weights of hormonal glands[2]. Figure 8 shows the correspondence of their weights with the main attractors. As an example let's analyze the weight of the hypophysis that statistically is around 500 mg:

$$\ln\left(\frac{m_{\,\text{hypophysis}}}{m_{\,\text{proton}}}\right) = \ln\left(\frac{5 \cdot 10^{-4}\ \text{kg}}{1.672622 \cdot 10^{-27}\ \text{kg}}\right) = 54$$

As you can see, the weight of the hypophysis coincides with the main attractor P[54] of proton stability. Doesn't this correlation remind you of something? Right, the main frequency of Theta brain activity coincides with the same attractor P[−54] of proton stability! The minus sign isn't significant — it changes to plus if you switch numerator and divisor.

In human EEG studies, the term "Theta" refers to frequency components in the 4–7 Hz range, regardless of their source. Indeed, due to the density of its neural layers, the hippocampus generates some of the strongest EEG signals of any brain structure, known as the hippocampal Theta rhythm.[3]

[1] Müller H. Astrobiological Aspects of Global Scaling. *Progress in Physics*, issue 1, 3–6, 2018.

[2] The GS-analysis of endocrine glands was made by doctor Leili Khosravi.

[3] Buzsaki G. Theta Oscillations in the Hippocampus. *Neuron*, vol. 33, 2002.

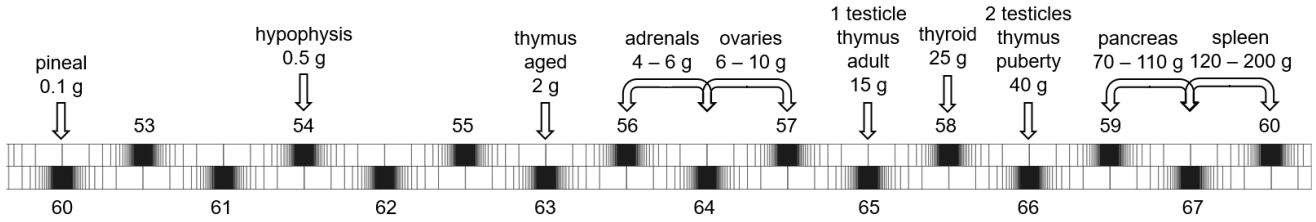

Figure 8: The weights of glands and their correspondence with attractors of electron (bottom) and proton (top) stability.

In vertebrate anatomy, the pituitary gland, or hypophysis, is a protrusion off the bottom of the hypothalamus at the base of the brain. One of the most important functions of the hypothalamus is to link the nervous system to the endocrine system via the pituitary gland.

The hypophysis is often referred to as the "master gland", because it controls several of the other hormone glands (adrenals, thyroid) and many biological functions: metabolism, growth, sexual activity, pregnancy, childbirth, nursing, blood pressure, temperature regulation, pain relief and stress response.

Do you remember the wavelengths corresponding to the Theta frequency range? It's easy to calculate: The main Theta frequency is 5 Hz, and the speed of light is nearly 300,000 km/s. Consequently, the wavelength is 300,000/5 = 60,000 km. This wavelength is in the scale of the body radii of Jupiter and Saturn, the largest and most massive planets, the "master planets" of the solar system. As you remember, we discovered already that the radius of Saturn coincides with the main attractor P[54] of proton stability (p. 39).

The coincidence of the Theta rhythm, the mass of the hypophysis and the radius of Saturn with the same main attractor P[54] of proton stability demonstrates how the FF connects processes of very different nature and scales. Interscalar connections are one of the most important features of the FF.

These connections are caused by the attractors of stability. If the frequency of some process coincides with an attractor of proton stability, then this frequency has a transcendental ratio to the natural frequency of the proton and consequently, it remains stable because it avoids proton resonance. Indeed, if the frequencies of two or more processes coincide with the same attractor of proton stability, the resonance probability between those processes increases and facilitates the communication between those processes. In this way, the attractors of proton and electron stability create stable channels of interscalar communication between processes which can be of very different scales.

Global Scaling explains the universe in terms of quantum oscillations and their stability. In the case of quantum oscillators like proton and electron, their metric characteristics are directly connected with frequencies through fundamental physical constants — the speed of light and the Planck constant. Therefore, the ratios of velocities, accelerations, energies or masses can be attributed to ratios of frequencies and expressed in terms of resonance and communication probability as well.

Some of the illustrious interscalar connections we already discussed in this book: between the human brain mass and the mass of the Sun;

between the focal length of the human eye and the radius of the photosphere of the Sun; between the size of the human zygote and the radius of Saturn (pp. 39–41). Through the FF, biological processes are embedded in the giant network of interscalar connections in the universe. Let's discover some more of them.

The Solar mass coincides with the main attractor E[139] of electron stability that coincides with attractor P[131;2] of proton stability, because $139 - 7\ \frac{1}{2} = 131\ \frac{1}{2}$. Dividing the logarithm $131.5/2 = 65.75$ we receive a logarithm that corresponds to the significant sub-attractor P[66;−4] in the range of the global average adult human body mass: $m_p \cdot \exp(65.75) = 60$ Kg.

In this way, the human brain mass is connected with the Sun's mass through the attractor E[139] of electron stability whereas the human body mass is connected with the Sun's mass through the attractor P[131;2] of proton stability. Consequently, the logarithm of the human body-to-brain mass ratio is exactly one half of the logarithm of the proton-to-electron mass ratio:

$$2 \ln\left(\frac{m_{\,\text{human body}}}{m_{\,\text{human brain}}}\right) = \ln\left(\frac{m_{\,\text{proton}}}{m_{\,\text{electron}}}\right)$$

This equation you can rewrite in the form:

$$\left(\frac{m_{\,\text{human body}}}{m_{\,\text{human brain}}}\right)^2 = \frac{m_{\,\text{proton}}}{m_{\,\text{electron}}}$$

Jupiter's body mass corresponds with the main attractor E[132] of electron stability:

$$\ln\left(\frac{M_{\,\text{Jupiter}}}{m_{\,\text{electron}}}\right) = \ln\left(\frac{1.8986 \cdot 10^{27}\ \text{kg}}{9.109383 \cdot 10^{-31}\ \text{kg}}\right) = 132$$

This attractor coincides with the attractor P[124;2] of proton stability, because $132 - 7\ \frac{1}{2} = 124\ \frac{1}{2}$. The half value of this logarithm $124.5/2 = 62.25$ corresponds to $m_p \cdot \exp(62.25) = 1.8$ kg that is the average weight of the adult human liver. It is remarkable that the most massive planet of the solar system corresponds with the most massive organ of the human organism — the liver:

$$\left(\frac{m_{\,\text{human liver}}}{m_{\,\text{proton}}}\right)^2 = \frac{M_{\,\text{Jupiter}}}{m_{\,\text{proton}}}$$

Considering the difference of the logarithms $139 - 132 = 7$ of the Sun's mass and Jupiter's mass, you can express the average mass of the human

liver also in units of the Sun's mass. Saturn's body mass is near the sub-attractor P[123;4] of proton stability:

$$\ln\left(\frac{M_{\text{ Saturn}}}{m_{\text{ proton}}}\right) = \ln\left(\frac{5.6836 \cdot 10^{26}\text{ kg}}{1.672622 \cdot 10^{-27}\text{ kg}}\right) = 123 + \frac{1}{4}$$

The half value of this logarithm $123.25/2 = 61.625$ corresponds to $m_p \cdot \exp(61.625) = 0.97$ kg that is the average weight of the adult human lungs. It is remarkable that the second massive planet of the solar system corresponds with the second massive organ of the human organism — the lungs:

$$\left(\frac{m_{\text{ human lungs}}}{m_{\text{ proton}}}\right)^2 = \frac{M_{\text{ Saturn}}}{m_{\text{ proton}}}$$

Now you can imagine that aliens who know Global Scaling and have studied the solar system can predict the human anatomy — at least the average weight of the human body, of its brain and the main organs including the glands, the size of the human zygote and the focal length of the human eye, the frequency ranges of the brain activity, the heart beat and breathing rates. Indeed, that's not all they can predict, as we will see soon.

The average birth weight of a full-term newborn is typically in the range of 2.5–5 kg[1]. The absolute record is 6.02 kg. These newborn body weights cover the range between the main attractors E[70] and E[71] of electron stability:

$$\ln\left(\frac{6\text{ kg}}{m_{\text{ electron}}}\right) = 71$$

$$\ln\left(\frac{2.5\text{ kg}}{m_{\text{ electron}}}\right) = 70$$

The average birth weight of babies in Europe is 3.6 kilograms and corresponds with the main attractor P[63] of proton stability:

$$\ln\left(\frac{3.6\text{ kg}}{m_{\text{ proton}}}\right) = 63$$

The logarithm 63 is exactly one half of the logarithm of the Venus-to-electron mass ratio that coincides with the main attractor E[126] of

[1] Janssen P. A. et al. Standards for the measurement of birth weight, length and head circumference at term in neonates of European, Chinese and South Asian ancestry. *Open Medicine*, vol. 1 (2), e74–e88, 2007.

electron stability:

$$\ln\left(\frac{M_{\text{Venus}}}{m_{\text{electron}}}\right) = \ln\left(\frac{4.8675 \cdot 10^{24}\ \text{kg}}{9.109383 \cdot 10^{-31}\ \text{kg}}\right) = 126$$

Consequently, our aliens which know the FF and have studied the solar system would know also the average human newborn body weight.

The average brain mass of full-term newborns is in the range of 350 g corresponding with the main attractor E[68] of electron stability:

$$\ln\left(\frac{0.35\ \text{kg}}{m_{\text{electron}}}\right) = 68$$

The average total body length 33–55 cm of full-term newborns is between the main attractor P[35] of proton stability and the main attractor E[28] of electron stability:

$$\ln\left(\frac{0.55\ \text{m}}{\lambda_{\text{electron}}}\right) = 28$$

$$\ln\left(\frac{0.33\ \text{m}}{\lambda_{\text{proton}}}\right) = 35$$

By the way, the normal head circumference for a full-term infant is 33–35 cm at birth.

Now let's analyze the average adult human body height[1]. Currently it is in the range of 147 cm (Guatemala, Bangladesh) to 186 cm (Bosnia and Herzegovina). The shortest adult human was recorded in Nepal at 55 cm. Its noticeable that his body height coincides with the maximum body length of a newborn. The tallest woman in medical history was recorded in China, who stood 248 cm when she died at the age of 17. The tallest living man is recorded in Turkey, at 251 cm:

$$\ln\left(\frac{2.5\ \text{m}}{\lambda_{\text{proton}}}\right) = 37$$

$$\ln\left(\frac{1.5\ \text{m}}{\lambda_{\text{electron}}}\right) = 29$$

Obviously, the adult human body height is between the main attractor E[29] of electron stability and the main attractor P[37] of proton stability.

[1]Krul A. J. et al. Self-reported and measured weight, height and body mass index (BMI) in Italy, the Netherlands and North America. *European Journal of Public Health*, vol. 21, 414–419, 2010.

If now we put together all ranges of the human body height — from the newborn minimum to the adult maximum, then it covers the range between the main attractors P[35] and P[37] of proton stability. The main attractor P[36] represents the logarithmic mean of this range that corresponds with the body height of $2.103089 \cdot 10^{-16} \cdot \exp(36) = 90$ cm that is typical for children in the age of 2 years. In this age, the baby becomes a toddler. This development stage is accompanied by a peak in the brain growth[1], enormous language improvements, accelerated learning and self-awareness.

And so, the human body height covers the range P[36±1] of proton stability. The double logarithm $36 + 36 = 72$ corresponds with Jupiter's surface gravity that coincides with the main attractor $[-72]$ of proton stability, as we have seen on page 31. That's another example of how biometrics is embedded in the solar system.

It is remarkable that many species develop body sizes and weights which coincide with main attractors of the FF. In 1981, the biologist Čislenko[2] discovered that the adults of various species prefer always the same quite narrow ranges of body sizes. These ranges show an equidistant logarithmic distribution. Čislenko estimated the scaling factor that connects one range with the next being close to 3. He analyzed the adult body sizes of ca. 4700 species of mammals, 5000 species of reptiles, 740 species of fish, 690 species of birds, 21000 species of insects and 900 species of bacteria.

Scale invariance as a property of the metric characteristics of biological organisms is well studied[3] and it is not an exclusive characteristic of adult physiology. In 1982, Zhirmunski and Kuzmin[4] discovered scaling in the sequence of the development stages in embryo-, morpho- and ontogenesis and supposed Euler's number being the scaling factor.

Within the current paradigm in biology, the phenomenon of generally preferred body sizes is difficult to explain. Why should it be equally advantageous for adult fish, amphibians, reptiles, birds and mammals of thousands of species to have body sizes always in the same ranges?

Čislenko assumed that in the realm of animals and plants there is not only a competition for food, water or other resources, but also a

[1] Knickmeyer R. C. et al. A structural MRI study of human brain development from birth to 2 years. *The Journal of Neuroscience*, vol. 28(47), 12176–12182, 2008.

[2] Čislenko L. L. The Structure of the Fauna and Flora in connection with the sizes of the organisms. Moscow, 1981.

[3] Schmidt-Nielsen K., Scaling. Why is the animal size so important? Cambridge University Press, 1984.

[4] Zhirmunsky A. V., Kuzmin V. I. Critical levels in developmental processes of biological systems. Moscow, Nauka, 1982.

struggle for a favorable body size. Each species tries to occupy an "advantageous" section on the logarithmic scale, whereby the mutual competitive pressure creates "crash zones". However, why both the "crash zones" and the overpopulated sections on the logarithmic scale are always of the same width, have the same distance from each other and why only certain ranges of body sizes are advantageous for the survival of the species and what these advantages are, could not be clarified. There are many studies confirming scaling in biology, although the deep causes have so far remained undiscovered.

Let us take a moment to think about this. The basic idea of Global Scaling is that the number continuum already contains the solution for lasting stability in systems of any degree of complexity. Therefore, it is not necessary to discover this solution by chance through a chaotic search by competition struggle. The solution is given a priori and it is omnipresent.

Another examples are the boundaries of the brain activity frequency ranges Theta, Alpha and Beta, which coincide with main attractors of the FF and are common for all mammals. We are talking not exclusively about human physiology, but about biophysics[1] as a whole.

Because of the universality of the FF, Schumann resonances[2] coincide with attractors which define also the boundaries of brain activity frequency ranges Theta, Alpha and Beta. This coincidence demonstrates that the electromagnetic activity of biological systems is embedded in the electromagnetic activity of the Earth. Furthermore, this coincidence allows for interscalar communication, that is, sharing of information between processes of different scales.

Let's analyze the Schumann resonances, starting with the fundamental mode of 7.83 Hz:

$$\ln\left(\frac{\omega_{\text{Schumann 1}}}{\omega_{\text{electron}}}\right) = \ln\left(\frac{7.83\ \text{Hz}}{7.763441 \cdot 10^{20}\ \text{Hz}}\right) = -46.04$$

Variations of the resonance frequencies can be caused by solar X-ray bursts[3]. In this case, the resonance frequency increases up to 8.2 Hz reaching the main attractor point E[−46] of electron stability. The

[1] Müller H. Chain Systems of Harmonic Quantum Oscillators as a Fractal Model of Matter and Global Scaling in Biophysics. *Progress in Physics*, issue 4, 231–233, 2017.

[2] Schumann, W. O. Über die strahlungslosen Eigenschwingungen einer leitenden Kugel, die von einer Luftschicht und einer Ionosphärenhülle umgeben ist. *Zeitschrift für Naturforschung A*, Bd. 7 (2), 149–154, 1952.

[3] Roldugin V. C. et al. Schumann resonance frequency increase during solar X-ray bursts. *Journal of Geophysical Research*, vol. 109, A01216, 2014.

frequency 14 Hz of the 2nd mode coincides with the main attractor P[−53] of proton stability:

$$\ln\left(\frac{\omega_{\text{Schumann 2}}}{\omega_{\text{proton}}}\right) = \ln\left(\frac{14\text{ Hz}}{1.425486\cdot 10^{24}\text{ Hz}}\right) = -52.99$$

It is remarkable that solar activity affects this mode much less or does not affect it at all. Indeed, the 3rd mode frequency 20.3 Hz must increase up to 22.2 Hz for reaching the main attractor point E[−45] of electron stability:

$$\ln\left(\frac{\omega_{\text{Schumann 3}}}{\omega_{\text{electron}}}\right) = \ln\left(\frac{20.3\text{ Hz}}{7.763441\cdot 10^{20}\text{ Hz}}\right) = -45.09$$

Schumann resonance modes can reach frequencies up to 60 Hz coinciding with the main attractor E[−44] of electron stability:

$$\ln\left(\frac{\omega_{\text{Schumann max}}}{\omega_{\text{electron}}}\right) = \ln\left(\frac{60\text{ Hz}}{7.763441\cdot 10^{20}\text{ Hz}}\right) = -44$$

The electromagnetic activity of biological systems is not only embedded in the electromagnetic activity of the Earth, but also in that of the Sun. It is notable that interscalar communication is not limited to low frequencies, but concerns also biophysics of light. For instance, the boundary between ultraviolet B and C light is close to the wavelength 280 nm that coincides with the main proton attractor P[21]:

$$\ln\left(\frac{\lambda_{\text{UV B−C}}}{\lambda_{\text{proton}}}\right) = \ln\left(\frac{2.8\cdot 10^{-7}\text{ m}}{2.103089\cdot 10^{-16}\text{ m}}\right) = 21$$

The essential for animals aromatic amino acids like tryptophan[1] have a peak of absorption at the wavelength 280 nm. You remember, this is also the size of the smallest living cells, the mycoplasma (p. 35).

The boundary between infrared B and C light is close to the wavelength 3.4 μm that coincides with the main electron attractor E[16]:

$$\ln\left(\frac{\lambda_{\text{IR B−C}}}{\lambda_{\text{electron}}}\right) = \ln\left(\frac{3.4\cdot 10^{-6}\text{ m}}{3.861593\cdot 10^{-13}\text{ m}}\right) = 16$$

A note on attractor points: As you can see in figure 2 on page 17, near an attractor point, the FF increases its density and in the point

[1] Yashchuk V. et al. Optical Response of the Polynucleotides-Proteins Interaction. *Molecular Crystals and Liquid Crystals*, vol. 535, 2011, issue 1, 93–110.

compression changes to decompression. This inversion has real consequences.

For example, UV B and C exhibit different properties of their interaction with atoms or molecules. The same is valid for IR B and C. In this way, FF-attractors mark not only islands of stability, but also points of change. Also the boundaries of the brain activity frequency ranges Theta, Alpha and Beta which coincide with main attractors of the FF, are points where the brain activity changes.

The change of compression to decompression near attractor points of the FF can have very different consequences. In geology, main equipotential surfaces of the FF coincide with shells of the Earth's interior where seismic waves change their velocity dramatically indicating sharp density boundaries.[1]

The propagation speed of seismic compression waves depends on the density and elasticity of the medium and therefore we can expect that they correspond with zones of compression and decompression near the main equipotential surfaces of the FF.

Figure 9 shows the linear 2D-projection of the FF in the interval between the main equipotential surface P[49] and the equipotential subsurface P[52;−4] of proton stability. At the graphic's left side the corresponding radii in km are indicated. The radial distribution of equipotential surfaces represents the 2D-profile of the Earth's interior the FF is suggesting. The minimum and maximum values of the Earth's radius approximate the equipotential surface E[44;4] of electron stability:

$$\ln\left(\frac{r_{\,\text{Earth max}}}{\lambda_{\,\text{electron}}}\right) = \ln\left(\frac{6.384\cdot 10^{3}\ \text{m}}{3.861593\cdot 10^{-13}\ \text{m}}\right) = 44.252$$

$$\ln\left(\frac{r_{\,\text{Earth min}}}{\lambda_{\,\text{electron}}}\right) = \ln\left(\frac{6.353\cdot 10^{3}\ \text{m}}{3.861593\cdot 10^{-13}\ \text{m}}\right) = 44.247$$

Figure 9 on the next page shows this attractor as dotted line in the top of the graphic.

Detailed seismic studies have shown that the speed of seismic P-waves (longitudinal pressure waves) in the mantle increases rather rapidly from about 9 to 11 km/s at depths between about 400 and 700 km, marking a layer called the transition zone. This zone separates the upper mantle from the lower mantle.

[1] Müller H. Quantum Gravity Aspects of Global Scaling and the Seismic Profile of the Earth. *Progress in Physics*, issue 1, 41–45, 2018.

In the FF, this transition zone corresponds with the compression zone before the sub-attractor P[52;−3] at a the distance of 5770 km from the Earth's center.

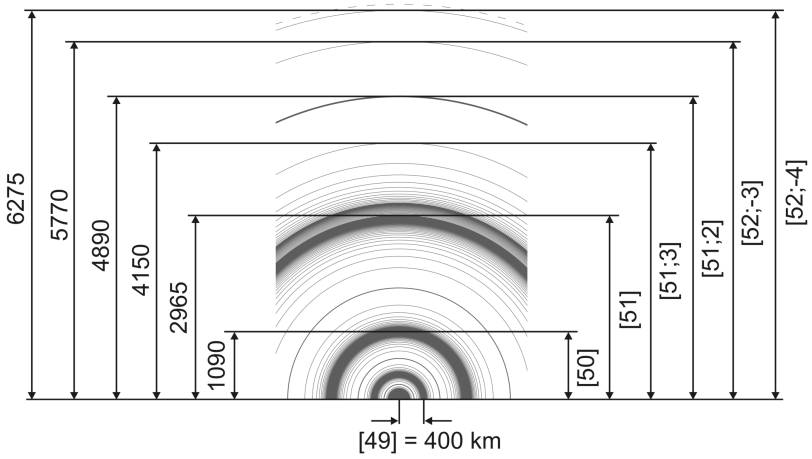

Figure 9: The Fundamental Field with equipotential surfaces of proton stability in the linear 2D-projection for $k = 1$ in the interval [49] ... [52;−4]. Radius in km (left side). The dotted line at the top indicates the Earth surface that coincides with the equipotential surface E[44;4] = 6372 km of electron stability.

As they travel more deeply into the mantle, P-waves increase their speed from 8 km/s at the Mohorovicic discontinuity to about 13 km/s at a depth of 2900 km. Once P-waves penetrate below 2900 km, their velocity suddenly drops from 13 km/s back down to about 8 km/s.

This dramatic reduction in speed at the depth of 2900 km defines the boundary between the Earth's mantle and the core. The outer core seems liquid, because seismic S-waves (transversal shear waves) do not pass this boundary. In contrast, the innermost part of the core within a radius of 1250 km seems solid. Reaching the inner core, P-waves again jump to a velocity of 11 km/s.[1]

Both standard models PREM[2] and IASP91[3] identify these bound-

[1]Kennett B. L., Engdahl E. R. Travel times for global earthquake location and phase identification. *Geophysical Journal International*, vol. 105, 429–465, 1991.

[2]Dziewonski A. M., Anderson D. L. Preliminary reference Earth model. *Physics of the Earth and Planetary Interiors*, vol. 25, 297–356, 1981.

[3]Kennett B. L. N. IASPEI 1991 Seismological Tables. Canberra, 1991.

aries with the radius of the liquid core (3480 km) and the radius of the inner solid core (1250 km). These estimations correspond with the compression zones before the main equipotential surfaces P[51] and P[50] and confirm that P-waves increase their velocity in the compression zone before the attractor. Then in the decompression zone, after the attractor, they decrease the velocity.

The pure compression zone of an attractor of proton stability begins always after the equipotential sub-surface $[n0; \pm 6]$ that coincides with the equipotential sub-surface $[n0; \pm 3]$ of electron stability, because $1/2 - 1/3 = 1/6$ (see figure 3 on page 22). The sub-surface P[51;6] of proton stability returns the radius 3500 km and the sub-surface P[50;6] has the radius 1290 km. This coincidence is a strong confirmation of the FF and suggests that the physical characteristics of the Earth's interior stratification are not casual, but an essential condition of its stability.

In accordance with the FF, the inner core should also have a substructure that originates from the equipotential surface P[49] at the distance of 400 km from the center. The compression zone of this attractor begins with the distance of P[49;6] = 475 km from the center. In fact, the seismological exploration of the Earth's inner core has revealed unexpected structural complexities. There is a well-defined hemispherical dichotomy in anisotropy and also evidence of a subcore with a radius 300–600 km.[1]

The FF predicts two additional zones of change which correspond with the equipotential surfaces P[51;3] of 4150 km radius and P[51;2] of 4890 km radius. The standard models PREM and IASP91 don't mention these peculiarities. Maybe they will be discovered.

Now let's pay attention to another interscalar connection: Whereas the radius of the Earth's subcore corresponds with the equipotential surface P[49] of proton stability, the radius of the Sun coincides with the same equipotential surface E[49], but of electron stability. So we can write down the equation for the ratio of the radii:

$$\frac{r_{\,\mathrm{Sun}}}{r_{\,\mathrm{Earth\,subcore}}} = \frac{\lambda_{\,\mathrm{electron}}}{\lambda_{\,\mathrm{proton}}}$$

In this example you can see how the knowledge of the FF allows for the discovery of interscalar connections which no one could imagine before. The electron-to-proton ratio we can find many times in the solar system. Let me give one more example.

[1] Deguen R. Structure and dynamics of Earth's inner core. *Earth and Planetary Science Letters*, vol. 333–334, 211–225, 2012.

As you already know, Saturn's body radius coincides with the main equipotential surface P[54] of proton stability (p. 39). At the same time, Venus' mean orbital distance coincides with the same equipotential surface E[54], but of electron stability (p. 30). Therefore, we can write down the equation:

$$\frac{R_{\,\text{Venus}}}{r_{\,\text{Saturn}}} = \frac{\lambda_{\,\text{electron}}}{\lambda_{\,\text{proton}}}$$

Talking about the radius of the Sun or that of a gas giant like Saturn, there is no solid surface connected with it. The visible diameter of the Sun is its photosphere whereas the visible diameter of Saturn is the boundary of its atmosphere or more precisely its stratosphere. This fact leads to the suggestion that the FF is forming the stratification of planetary and stellar atmospheres as well. Let's check this idea and analyse the stratification of the Earth's atmosphere.

The vertical stratification of the Earth's atmosphere is caused by very different processes and it is a complex field of research. In general, air pressure and density decrease exponentially with altitude, but temperature, ionization and chemical composition have more complicated profiles.

The standard division into troposphere, stratosphere, mesosphere, thermosphere, ionosphere and exosphere is based on satellite, airplane and ground measurements and considers aerodynamic, hydrodynamic, thermodynamic, electromagnetic, chemical and gravitational factors in their complex interaction.

Stratification as atmospheric feature is associated not only with the Earth, but occurs on any other planet or moon that has an atmosphere as well. Furthermore, stable atmospheric boundaries like tropopause, stratopause, thermopause and mesopause have similar vertical distributions at different celestial bodies in atmospheres of very different chemical compositions.

Being gas, the atmosphere is bounded by the lithosphere and the hydrosphere of the planet. The lowest layer of Earth's atmosphere is the troposphere where nearly all weather conditions take place. The average height of the troposphere[1] is 20 km in the tropics, 12 km in the mid latitudes, and 7 km in the polar regions in winter. Table 3 and figure 10 show the correspondence of these tropospheric levels with the equipotential surfaces E[37;2], E[38] and E[38;2] of electron stability.

At its lowest part, the planetary boundary layer (PBL), the troposphere displays turbulence and strong vertical mixing due to the contact

[1] Danielson, Levin, Abrams. Meteorology. McGraw Hill, 2003.

with the planetary surface. The top of the PBL[1] in convective conditions is often well defined by the existence of a stable capping inversion, into which turbulent motions from beneath are generally unable to penetrate.

The height of this elevated stable layer is quite variable, but is generally below 3 km. Over deserts in mid-summer under strong surface heating the PBL may rise to 4–5 km. In the temperate zones, it can be defined by the quite sharp decrease of aerosol concentration at the height of about 1600 m. Over the open oceans, but also at night over land, under clear skies and light winds, with a capping stratocumulus, the depth of the PBL may be no more than 600 m.

Table 3 shows the correspondence of the PBL features with the main equipotential surfaces E[35], E[36] and E[37] of electron stability. Above the PBL, where the wind is nearly geostrophic, vertical mixing is less and the free atmosphere density stratification begins.

The jet stream flows near the boundary between the troposphere and the stratosphere. As altitude increases, the temperature of the troposphere generally decreases until the tropopause.

At the bottom of the stratosphere, above the tropopause, the temperature doesn't change much, but at the inverse layer at altitudes between 20 and 33 km the temperature increases from -50°C to 0°C. Then at the stratopause at 55 km altitude the temperature stabilizes. The stratopause is the boundary between two layers: the stratosphere and the mesosphere[2].

The ozone layer (ozonosphere) of the stratosphere absorbs most of the Sun's ultraviolet radiation and is mainly found at altitudes between 12 and 30 km, with the highest intensity of formation at 20 km height[3]. Figure 10 shows the correspondence of the main stratosphere layers with the equipotential surfaces E[39] and E[39;2] of electron stability[4].

Above the stratopause, in the mesosphere between 55 and 90 km altitude[5], the temperature decreases again, reaching about -100°C at

[1] Garratt J. R. Review: The atmospheric boundary layer. *Earth-Science Review*, vol. 37, 89–134, 1994.

[2] Brasseur G. P., Solomon S. Aeronomy of the Middle Atmosphere. Chemistry and Physics of the Stratosphere and Mesosphere. Springer, 2005.

[3] Stolarski R. et al. Measured Trends in Stratospheric Ozone. *Science*, New Series, vol. 256, issue 5055, 342–349, 1992.

[4] Müller H. Global Scaling of Planetary Atmospheres. *Progress in Physics*, issue 2, 66–70, 2018.

[5] Holton J. R. The Dynamic Meteorology of the Stratosphere and Mesosphere. Meteorological monograph, vol. 15, no. 37, American Meteorological Society, Boston (Massachussetts), 1975.

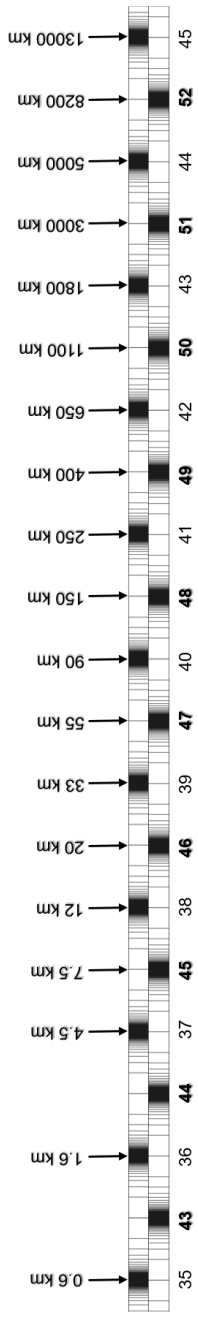

Figure 10: Altitudes (top) of atmospheric stratification boundaries and their correspondence with equipotential surfaces of proton (lower FF) and electron (upper FF) stability (logarithmic scale).

BOUNDARY	ALTITUDE h, KM	$\ln(h/\lambda_e)$	FF
van Allen outer electron belt	13000	44.96	E[45]
	8200		E[44;2]
	5000		E[44]
van Allen inner proton belt	3000	43.50	E[43;2]
Earth exopause	1800	42.99	E[43]
	1100		E[42;2]
Earth thermopause	650	41.97	E[42]
	400		E[41;2]
Venus & Mars thermopause Venus atmospheric entry	250	41.01	E[41]
Earth atmospheric entry Venus mesopause	150	40.50	E[40;2]
Earth & Titan mesopause Venus tropopause Mars stratopause & entry	90	39.99	E[40]
Earth & Titan stratopause	55	39.50	E[39;2]
Titan tropopause	33	38.99	E[39]
Earth tropic tropopause	20	38.49	E[38;2]
Earth temperate tropopause	12	37.98	E[38]
Earth polar tropopause	7.5	37.51	E[37;2]
desert summer PBL inversion	4.5	37.00	E[37]
continental PBL inversion	1.6	35.96	E[36]
marine PBL inversion	0.6	34.98	E[35]

Table 3: The atmospheric stratification boundaries on Earth, Venus, Mars and Titan and their correspondence with equipotential surfaces of electron stability.

the mesopause[1]. The mesopause corresponds with the main equipotential surface E[40] of electron stability. This altitude of 90 km coincides with the turbopause: above this level the atmosphere is of extremely low density so that the chemical composition is not mixed but stratified and depends on the molecular masses.

Above the mesopause, in the thermosphere, the (kinetic) temperature increases and can rise to 1000°C (depending on solar activity) at altitudes of 250 km remaining quasi stable with increasing height. Due to solar radiation, gas molecules dissociate into atoms: above 90 km carbon dioxygen and dihydrogen dissociate, above 150 km dioxygen dissociates and above 250 km dinitrogen dissociates. Above 150 km, the density is so low that molecular interactions are too infrequent to permit the transmission of sound. These thermospheric layers correspond with the main equipotential surfaces E[40;2] and E[41] of electron stability.

The Karman line[2] is considered by the Federation Aeronautique Internationale (FAI)[3] as the border between the atmosphere and outer space, as altitude where the atmosphere becomes too thin to support aeronautical flight, since a vehicle at this altitude would have to travel faster than orbital velocity to derive sufficient aerodynamic lift to support itself.

On Earth, atmospheric effects become noticeable during atmospheric entry of spacecraft already at an altitude of around 120–150 km, while on Venus the atmospheric entry occurs at 250 km and on Mars at about 80–90 km above the surface. These heights mark also the bases of the anacoustic zones where the density of the atmosphere is too low for sound propagation.

The location of the thermopause is near altitudes of 600 – 700 km and depends on solar activity[4]. The thermopause corresponds with the main equipotential surface E[42] of electron stability. Above starts the exosphere, where the atmosphere (mostly consisting of hydrogen atoms) thins out and merges with interplanetary space. This uppermost layer, until 13,000 km observable from space as the geocorona, extends up to 100,000 km.

---

[1]Beig G., Keckhut P. Lowe R. P. et al. Review of mesospheric temperature trends. *Rev. Geophys.*, vol. 41 (4), 1015, 2003.

[2]Karman T., Edson L. The Wind and Beyond. Little, Brown, Boston, 1967.

[3]Cordoba S. F. The 100 km Boundary for Astronautics. Federation Aeronautique Internationale, 2011.

[4]Beig G., Scheer J., Mlynczak M. G., Keckhut P. Overview of the temperature response in the mesosphere and lower thermosphere to solar activity. *Reviews of Geophysics*, vol. 46, RG3002, July 2008.

The van Allen[1] radiation belts are features of Earth's magnetosphere. The inner belt consists of high energetic protons which reach their maximum concentration at altitudes of 3,000 km. The outer belt consists of high energetic electrons with maximum concentration at altitudes of 13,000 km. The outer belt maximum corresponds well with the main equipotential surface E[45] of electron stability, but the inner belt maximum corresponds with the equipotential surface E[43;2] that is the main equipotential surface P[51] of proton stability. In this way, the FF delivers not only a correct estimation of their altitudes, but also a simple explanation of the separation in two belts of high proton and high electron concentration respectively.

Probably, in future the FF can be applied for estimation of the atmospheric stratification at ice giants like Uranus and Neptune and gas giants like Jupiter, Saturn and extrasolar planets as well. Vacant attractors in table 3 could be identified as stratification features.

Having analysed the solar system, now we venture into more distant regions of the Milky Way (MW), our home Galaxy. At the same time, we have to consider that distance measurement by parallax triangulation is precise enough only up to 500 light years. With the increase of the distances, indirect methods are applied blurring the difference between facts and model claims.

Furthermore, all 300 or more billions of stars in the Galaxy are moving and changing their relative positions and distances continuously. Nevertheless, analysing the distances between stars with the help of the FF we can estimate the probability that a distance is currently stable or intensely changing. In this way, we can also get an idea about the hierarchy of the stars in a group. Of course, our estimation will be very hypothetical while it is not possible to verify by observation. Let's start with our star neighbourhood. The distance to the Sirius system 8.60(4) light years fits with the main attractor P[75] of proton stability,

$$\ln\left(\frac{R_{\,\mathrm{Sirius}}}{\lambda_{\,\mathrm{proton}}}\right)=\ln\left(\frac{8.6\cdot 0.946053\cdot 10^{16}\ \mathrm{m}}{2.103089\cdot 10^{-16}\ \mathrm{m}}\right)=75$$

whereas the distance to the Alpha Centauri system 4.34(3) light years coincides with the sub-attractor P[74;3]:

$$\ln\left(\frac{R_{\,\mathrm{Alpha\ Cen}}}{\lambda_{\,\mathrm{proton}}}\right)=\ln\left(\frac{4.3\cdot 0.946053\cdot 10^{16}\ \mathrm{m}}{2.103089\cdot 10^{-16}\ \mathrm{m}}\right)=74+\frac{1}{3}$$

[1]Schaefer H. J. Radiation Dosage in Flight through the Van Allen Belt. *Aerospace Medicine*, vol. 30, no. 9, 1959.

Knowing the sky coordinates of both Alpha Centauri and Sirius, it is possible to calculate the distance between them by triangulation[1]. However, in this book we will not. In general, single stars don't orbit each other if they are not members of the same system. However, we can expect that in general, stars orbit the Galactic Center (GC).

Currently there is no precise measurement of the distance to the Galactic Center, but 26,000 light years seems an accepted estimation[2] and it coincides with the main attractor P[83] of proton stability:

$$\ln\left(\frac{R_{\,\mathrm{Sun-GC}}}{\lambda_{\,\mathrm{proton}}}\right) = \ln\left(\frac{2.6\cdot 10^4\cdot 0.946053\cdot 10^{16}\ \mathrm{m}}{2.103089\cdot 10^{-16}\ \mathrm{m}}\right) = 83.05$$

If the current measurement is correct, it would mean that the solar system orbits the Galactic Center at a distance that avoids resonance interaction with it. Good for us. By the way, 26,000 years reminds us of the precession period of the Earth that coincides with the same, but temporal attractor P[83] of proton stability:

$$\ln\left(\frac{T_{\,\mathrm{Earth\,precession}}}{\tau_{\,\mathrm{proton}}}\right) = \ln\left(\frac{2.6\cdot 10^4\cdot 31558149.54\ \mathrm{s}}{7.015150\cdot 10^{-25}\ \mathrm{s}}\right) = 83.05$$

This coincidence of the precession period of the Earth with its distance to the Galactic Center isn't random, but indicates a profound connection of both processes given by the FF. Both processes are of the same scale, only in one case it is a spatial scale and in the other case it is a temporal scale and so they meet the same attractor.

Now let's look beyond our Galaxy at some members of the local group. It is easy to observe them even with a good binocular, but it is hard to measure the distances to them. They are too large for direct parallax triangulation. For determination of intergalactic distances, Cepheid variable stars in other galaxies are observed.

In 1908 Henrietta Swan Leavitt[3] who was looking for Cepheid stars in the Magellanic Clouds, discovered a period–luminosity relation for Cepheids. She found that Cepheids of a high brightness have larger pulsation periods than those of lower brightness. Thanks to this discovery, one can measure how often the Cepheid changes luminosity and calculate its intrinsic luminosity.

[1] Hirshfeld A. W. Parallax: The Race to Measure the Cosmos. Dover Publ., 2002.

[2] Groom D. E. et al. Astrophysical constants. *European Physical Journal C*, vol. 15, 1, 2000, www.pdg.lbl.gov

[3] Leavitt H. S. 1777 variables in the Magellanic Clouds. *Annals of Harvard College Observatory*, vol. 60, 87, 1908.

It is believed that for any star, its apparent luminosity (how bright it appears to us) decreases with the square of the distance to the observer. If now we measure the apparent luminosity of a Cepheid and we know its intrinsic luminosity by measuring its period, we can obtain the approximate distance to the object.

Indeed, some assumptions[1] need to be made before measuring distances using Cepheid stars: the period-luminosity relation of all Cepheids must be the same; all Cepheids of one galaxy must be equidistant from the Earth; their light must not be absorbed by dust clouds.

Considering the uncertainty of these assumptions, we should be careful with far-reaching interpretations of those measurements. However, for exercise let us consider them as trustable. Today the distance to the Large Magellanic Cloud (LMC) is estimated to be 186 thousand light years and it coincides with the attractor E[77;2] of electron stability:

$$\ln\left(\frac{R_{\mathrm{MW-LMC}}}{\lambda_{\mathrm{electron}}}\right) = \ln\left(\frac{1.86\cdot 10^5\cdot 0.946053\cdot 10^{16}\ \mathrm{m}}{3.861593\cdot 10^{-13}\ \mathrm{m}}\right) = 77.50$$

The distance to the Small Magellanic Cloud (SMC) is estimated with 157 thousand light years and it coincides with the attractor E[77;3] of electron stability:

$$\ln\left(\frac{R_{\mathrm{MW-SMC}}}{\lambda_{\mathrm{electron}}}\right) = \ln\left(\frac{1.57\cdot 10^5\cdot 0.946053\cdot 10^{16}\ \mathrm{m}}{3.861593\cdot 10^{-13}\ \mathrm{m}}\right) = 77.33$$

The Andromeda galaxy M31 seems to be at a distance of 2.5 million light years[2] that is in the deceleration zone after the last sub-attractor E[80;6] of both proton and electron stability, very close to the main attractor E[80] of electron stability:

$$\ln\left(\frac{R_{\mathrm{MW-M31}}}{\lambda_{\mathrm{electron}}}\right) = \ln\left(\frac{2.5\cdot 10^6\cdot 0.946053\cdot 10^{16}\ \mathrm{m}}{3.861593\cdot 10^{-13}\ \mathrm{m}}\right) = 80.10$$

For reaching the attractor E[80], the Andromeda-to-Milky Way distance has to decrease by 240 thousand light years down to 2.26 million light years:

$$3.861593\cdot 10^{-13}\ \mathrm{m}\cdot\exp(80) = 2.26\cdot 10^6\ \mathrm{ly}$$

They seem to do exactly this. M31 is approaching (more precisely, 2.5 million years ago was approaching) the Milky Way at about 100

[1] Casertano S. et al. Parallax of Galactic Cepheids. arXiv:1512.09371v2, 2016.

[2] Ribas I. et al. First Determination of the Distance and Fundamental Properties of an Eclipsing Binary in The Andromeda Galaxy. arXiv:astro-ph/0511045v1, 2005.

kilometers per second, as indicated by blueshift measurements[1]. If the velocity of approach is constant, the current distance to M31 should be already 1,000 light years shorter than the 2.5 million years old distance we can measure today.

Standard model calculations (naturally without consideration of the FF) expect that both galaxies will collide in a few billion years. Considering the fractality of the FF, we can expect that the approach velocity is slowly decreasing and after reaching the attractor E[80], the approach will be finished and the distance between both galaxies will be stabilized at 2.26 million light years. As you can see, the consideration of the FF can modify predictions completely.

Talking about galaxies, we can't avoid mentioning the hypothesis about dark matter. It is important for us to understand where this hypothesis is coming from and how it is related with the evidence of the FF. Hence, let's spend a few minutes on this topic.

Already in 1933, Fritz Zwicky[2] studied the Coma Cluster and obtained evidence of unseen mass that he called "dark matter". In 1957, Henk van de Hulst and then in 1959, Louise Volders demonstrated that the galaxies M31 and M33 do not spin as expected in accordance with Kepler's laws.

The orbital velocities of stars should decrease in an inverse square root relationship with the distance from the Galactic Center, similar to the orbital velocities of planets in the solar system. But this is not observed. Outside of the central galactic bulge the orbital velocities are nearly constant.

According to Newton's hypothesis of mass as source of gravity, this deviation might be explained by the existence of a substantial amount of matter flooding the galaxy that is not emitting light and interacts barely with ordinary matter and therefore it is not observed.

Here it is important to realize that dark matter is required only if mass causes gravitational interaction. Indeed, exactly this point is still under discussion.

The origin of gravity is a key topic in modern physics. Furthermore, gravity is the only interaction that is not described yet by a consistent quantum theory. The universality of gravity means that the free fall acceleration of a test body at a given location does not depend on its mass, physical state or chemical composition.

---

[1] Cowen R. Andromeda on collision course with the Milky Way. *Nature.com*, 31 May 2012.

[2] Zwicky F. On the Masses of Nebulae and of Clusters of Nebulae. *The Astrophysical Journal*, vol. 86, 217, 1937.

This discovery, made four centuries ago by Galileo Galilei, is confirmed by modern measurements with an accuracy of 10^{10}–10^{12}. A century ago Einstein supposed that gravity is indistinguishable from, and in fact the same thing as, acceleration. In fact, Earth's surface gravity acceleration g can be derived from the orbital elements of any satellite, also from the Moon's orbit:

$$\mu = 4\pi\frac{R^3}{T^2} = 3.9860044 \cdot 10^{14}\ \mathrm{m}^3/\mathrm{s}^2$$

$$g = \frac{\mu}{r^2} = \frac{\mu}{(6372000\ \mathrm{m})^2} = 9.82\ \mathrm{m}/\mathrm{s}^2$$

R is the semi-major axis of the Moon's orbit, T is the orbital period of the Moon and r is the average radius of the Earth, μ is called the geocentric gravitational constant. As you can see, no data about the mass or chemical composition of the Earth or the Moon is needed.

Kepler's 3rd law describes the ratio R^3/T^2 as constant for a given orbital system. Kepler's discovery is confirmed by high accuracy radar and laser ranging of the movement of artificial satellites. Kepler's 3rd law is of geometric origin and can be derived from Gauss's flux theorem in 3D-space. The law applies to all conservative fields which decrease with the square of the distance[1] and does not require the presence of mass.

Newton's law of universal gravitation postulates the identity $\mu = GM$, an interpretation that provides the mass M as source of gravity and the universality[2] of the big G. Both postulates are essential in Newton's theory of gravitation and in Einstein's general theory of relativity.

And yet, they are not essential for precise description and prediction of the orbital movements in the solar system. Therefore, Newton's hypothesis about mass as source of gravity could turn out to be a dispensable assumption.

In the case of mass as source of gravity, in accordance with Newton's shell theorem, a solid body with a spherically symmetric mass distribution should attract particles outside it as if its total mass were concentrated at its center. In contrast, the attraction exerted on a particle should decrease as the particle goes deeper into the body and it should become zero at the body's center.

[1] Wess J. Theoretische Mechanik. Springer, 2009.

[2] Quinn T., Speake C. The Newtonian constant of gravitation — a constant too difficult to measure? An introduction. *Phil. Trans. Royal Society A*, vol. 372, 20140253.

A boat at the latitude 86.71 and longitude 61.29 on the surface of the Arctic Ocean, would be at the location that is regarded as having the highest gravitational acceleration on Earth. At that location, the gravitational acceleration is 9.8337 m/s^2. At higher or lower position to the center of the Earth, gravity should be of less intensity. This conclusion seems correct, if only mass is the source of gravity acceleration and if the big G is universal under any conditions and in all scales.

The Preliminary Reference Earth Model[1] affirms the decrease of the gravity acceleration with depth. However, also this hypothesis is still under discussion.

In 1981–1986, Stacey[2], Tuck, Holding, Maher and Morris reported[3] anomalous measurements (larger values than expected) of the gravity acceleration in deep mines and boreholes. Frank Stacey writes: "Modern geophysical measurements indicate a 1% difference between values at 10 cm and 1 km (depth). If confirmed this observation will open up a new range of physics".[4]

Is it this new range of physics that you touch upon while reading this book? Like already many times in history, new physics is coming from mathematics developed centuries ago, but applied only today.

---

[1] Dziewonski A. M., Anderson D. L. Preliminary reference Earth model. *Physics of the Earth and Planetary Interiors*, vol. 25, 297–356, 1981.

[2] Stacey F. D. et al. Constraint on the planetary scale value of the Newtonian gravitational constant from the gravity profile within a mine. *Phys. Rev. D*, vol. 23, 1683, 1981.

[3] Holding S. C., Stacey F. D., Tuck G. J. Gravity in mines. An investigation of Newton's law. *Phys. Rev. D*, vol. 33, 3487, 1986.

[4] Stacey F. D. Gravity. *Science Progress*, vol. 69, no. 273, 1–17, 1984.

Nothing is Artificial in the Universe

> Every production, of whatever kind,
> is an alteration, but the substance
> remains always the same.
>
> *Giordano Bruno*

The basic idea of Global Scaling is that the solution for lasting stability in systems of any degree of complexity is an inherent feature of the number continuum given by the natural exponential function e^x for rational exponents. The solution is given a priori and it is omnipresent.

Naturally, this solution is available for technical systems too. Therefore, Global Scaling is significant in engineering as well. Analyzing a few striking examples, we will see that technology is sensitive to FF-attractors of stability.

Let's start with computer technology. One of the significant characteristics of microprocessors is the clock rate. Analyzing the development history of microprocessors, we can see that the most popular clock rates occupy main attractors of stability.

Figure 11 shows the distribution of the clock rates in MHz. In the top of the graphic you can see the frequency ranges applied to various generations of Intel processors[1].

A clock generator is an electronic oscillator circuit that uses the mechanical resonance of a vibrating crystal of piezoelectric material (quartz or ceramic) to create an electrical signal with a stable frequency. Manufacturers have difficulty producing crystals thin enough to generate fundamental frequencies over 30 MHz, so that high frequency crystals are often designed to operate at third, fifth, or seventh overtones. Please note that they are not integer multiples of the fundamental frequency.

FF-attractor frequencies are applied not only as clock rates in PCs, but also in USB-technology (6 MHz), GPS, DECT (10 MHz), 3G, EGA (16 MHz), VGA, GSM, UMTS (25 MHz), remote controlled cars and boats (40 MHz), Ethernet (50 MHz), PCI (66 MHz) and as carriers in FM radio (100 MHz), radio control (333 MHz), cell phone (900, 1400 MHz) and Wi-Fi (2.4 GHz).[2]

[1] Intel Microprocessor Quick Reference Guide — Product Family. www.intel.com
[2] Crystal oscillator frequencies. www.en.wikipedia.org

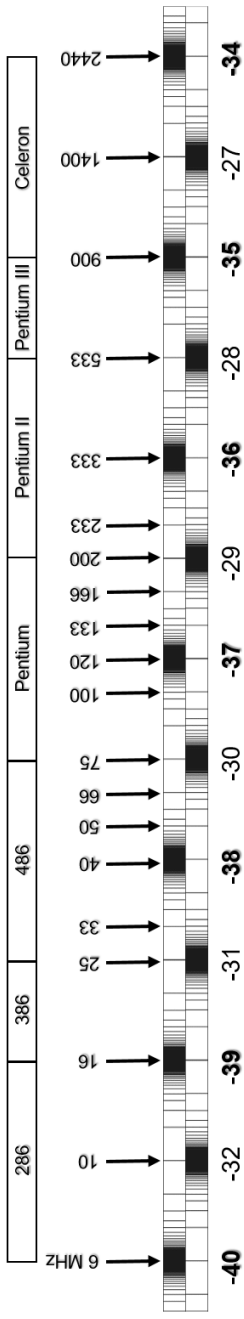

Figure 11: Clock rates (MHz) applied to Intel microprocessors and their correspondence with attractors of proton (bold) and electron (thin) stability. Data taken from: Intel Microprocessor Quick Reference Guide — Product Family.

The transition from frequencies to wavelengths of the proton or electron is given by the (constant) speed of light. Therefore, the logarithm changes only the sign, so that the frequency range between the proton attractors P[−37] = 120 MHz and P[−35] = 900 MHz corresponds to the range of wavelengths between P[35] = 33 cm and P[37] = 250 cm coinciding with the human body size range.

On the example of crystal oscillators, we have seen that FF-attractor islands of stability concern mechanical oscillations as well. Always when high precision stability is required, the preferred physical quantities in mechanical applications correspond with FF-attractors.

A striking example are the calibers of sportive guns, because of the advanced requirements to the precision and ballistic stability, and especially those of pneumatic construction, because of the applied modest initial impulse.

The most distributed caliber of sporting air rifles[1] is 4.5 mm (diameter), for use in international target shooting competition at 10 m, up to Olympic level in both rifle and pistol events. This type of riffles has helical grooves called rifling machined into the bore wall. When shooting, a rifled bore imparts spin to the projectile about its longitudinal axis, which gyroscopically stabilizes the projectile's flight.

Analyzing the rotation radius 4.5 mm/2 = 2.25 mm, we discover that it fits perfectly with the main attractor P[30] of proton stability:

$$\ln\left(\frac{2.25\cdot 10^{-3}\ \mathrm{m}}{\lambda_{\,\mathrm{proton}}}\right) = 30.00$$

The radius 3.8 mm of the prominent caliber 7.6 mm coincides with the main attractor E[23] of electron stability:

$$\ln\left(\frac{3.8\cdot 10^{-3}\ \mathrm{m}}{\lambda_{\,\mathrm{electron}}}\right) = 23.01$$

The proton Compton wavelengths equal: $\lambda_{\mathrm{proton}} = 2.103089\cdot 10^{-16}$ m and $\lambda_{\mathrm{electron}} = 3.861593\cdot 10^{-13}$ m (see table 1 on page 20).

I have no intention of going any deeper into the study of weapons. Naturally, it is more a question of ethics than of technology to find out how to prevent the misuse of technological advances against life. Yet, I do not wish to support any research in this field.

Instead, let's analyze some features of modern car technology. One of the most loaded part of the car construction and exposed to high wear

[1] Hoff A. Air-guns and Other Pneumatic Arms. Barrie & Jenkins, London, 1972.

is the wheel. Quietness under high speed rotation and mechanical stress requires a high level of stability avoiding internal resonance. Therefore, we can expect that significant physical characteristics of the most distributed constructions correspond with FF-attractors of stability. In fact, the most popular wheel size[1] in the USA and Europe is the R15. It is installed on 50% of passenger cars and light SUVs. Considering a fitting tire like 185/80-R15 or 205/75-R15, we always get a total wheel radius of about 34 cm that corresponds with the main attractor P[35] of proton stability:

$$\lambda_{\text{proton}} \cdot \exp(35) = 0.33 \text{ m}$$

As you can see, the unloaded dimension of the car tire is a little bit larger than the attractor point wavelength, so that the attractor point can be reached during the rotation under load. The requirements to aircraft tires[2] are even higher because of high acceleration by landing and high load capacity. For example, the B737 main gear tires are of the type H44.5x16.5-21, where 44.5 inches is the total diameter of the tire. Consequently, the radius of the tire is 22.25 inches = 56.5 cm that corresponds with the main attractor E[28] of electron stability:

$$\lambda_{\text{electron}} \cdot \exp(28) = 0.56 \text{ m}$$

Another highly loaded component is the internal combustion engine. That's why we are going to analyze some of its functionally significant physical characteristics. Lasting stability of the movement of the pistons with minimum friction losses under conditions of high temperature and high pressure requires high precision of manufacturing.

Furthermore, quietness is required, resonance vibrations are undesirable, so we can expect that the functional physical characteristics should be sensitive to attractors of proton or electron stability.

Regardless of any advanced electronic control, the undisputed law of combustion engines says: "There's no replacement for displacement." In fact, the engine displacement is functionally highly significant. Analyzing some widespread displacement volumes, we can see that obviously, already the volume by itself as physical quantity is sensible to attractors of proton or electron stability. For example, the famous 1.9-liter displacement coincides with the main attractor P[102].

$$\ln\left(\frac{1.86 \cdot 10^{-3}\,\text{m}^3}{\lambda_{\text{proton}}^3}\right) = 102$$

[1] The Most Popular Tire Sizes: R15. Capitol Tires. 2018.

[2] Aircraft Tire Dimensions: www.boeing.com; Global Aviation Tires: www.goodyearaviation.com; Aircraft Tire Engineering Data: www.michelinair.com

In fact, the physical displacement volume is a little bit less than 1.9 liters. The fundamental proton unit for volumes is $\lambda^3_{\text{proton}} = 9.3019276 \cdot 10^{-48}\,\text{m}^3$ (see table 1 on page 20).

Based on the prominent displacement volume 250 cm^3 all scooters[1] are divided in two classes — mini and maxi. You remember that FF-attractors are also points of change. This boundary volume coincides with the main attractor P[100]:

$$\ln\left(\frac{2.5 \cdot 10^{-4}\,\text{m}^3}{\lambda^3_{\text{proton}}}\right) = 100$$

Another significant characteristic is the speed of revolution that is for modern internal combustion (Diesel) engines between 800 (in neutral) and 6000 revolutions per minute. These limits correspond with the main attractors P[−53] respectively P[−51]:

$$\ln\left(\frac{(6000/60)\,\text{Hz}}{\omega_{\text{proton}}}\right) = -51$$

$$\ln\left(\frac{(800/60)\,\text{Hz}}{\omega_{\text{proton}}}\right) = -53$$

The angular frequency of the proton is $\omega_{\text{proton}} = 1.425486 \cdot 10^{24}$ Hz. Consequently, the logarithmic mean rotation speed of 2200/min coincides with the attractor P[−52] of stability:

$$\ln\left(\frac{(2200/60)\,\text{Hz}}{\omega_{\text{proton}}}\right) = -52$$

It is a small step from transport technology to traffic where the driving speed is a highly significant metric characteristic.

As fundamental characteristic of space-time, the speed of light is a common property of both proton and electron connecting their natural frequencies with the wavelengths. Consequently, the attractors of velocities are the same for proton and electron stability, so we use square brackets without E or P.

It is remarkable that also traffic tries to avoid resonance interaction and consequently, traffic is sensitive to FF-attractors of stability. For example, in many countries the traffic speed on highways is limited, mostly to 120 km/h that is also the average speed on highways in Germany where there is no speed limitation.[2] Naturally, the existence of a

[1] Scooter (motorcycle). www.en.wikipedia.org

[2] Kellermann G. Geschwindigkeitsverhalten im Autobahnnetz 1992. *Strasse und Autobahn*, issue 5, 1995.

limit pushes the drivers to go up to the limit, whenever it is possible. Therefore, it is important that the limit coincides with an attractor of stability. In the case of 120 km/h it really does:

$$\ln\left(\frac{(120/3.6)\,\mathrm{m/s}}{c}\right) = -16$$

The speed of light in vacuum is $c = 299,792,458$ m/s. For safety reasons, the maximum speed of tuned cars registered for public transport and also of ultralight aviation is limited to 330 km/h that is a main attractor and consequently, a boundary speed as well:

$$\ln\left(\frac{(330/3.6)\,\mathrm{m/s}}{c}\right) = -15$$

Statistically, the speed at high traffic levels on highways fluctuates around the average of 75 km/h. Trying to avoid collision, drivers empirically find this attractor of stability:

$$\ln\left(\frac{(75/3.6)\,\mathrm{m/s}}{c}\right) = -16 - \frac{1}{2}$$

Interestingly, the line of cars does not stand in the traffic jam, but moves backwards — it gets longer. The jam snake grows in the direction opposite the traffic flow[1] at an average of 15 kilometers per hour that coincides with the main attractor $[-18]$:

$$\ln\left(\frac{(15/3.6)\,\mathrm{m/s}}{c}\right) = -18$$

The adaption to a main attractor of stability is very understandable if we consider that physical resonance interaction in a traffic jam would provoke a disaster.

Here we can begin to see technology in general as not something artificially created by humans, but as a cosmic phenomenon. Probably, many other civilizations in the Galaxy create technology as well. However, all this technology is part of the universe, it isn't something unnatural, it consists of the same natural atoms and it is created by the universe itself — we are only the hands of the universe.

From the point of view of Global Scaling, there is nothing "artificial" in the universe. Everything, whether man-made or naturally grown,

[1] Verkehrsfluss und Stauaufkommen. Definitionen. Bundesamt für Strassen, ASTRA. Schweizerische Eidgenossenschaft. www.astra.admin.ch

must take into account the FF, because it defines the distribution of stability attractors in all scales of the universe.

As examples, let us remember also the seismic waves (p. 51) which change their velocities from 13 km/s = [−10] downto 8 km/s = [−10;−2] on the boundary between the Earth's mantle and the core. By the way, Jupiter's orbital velocity fits with the same main attractor [−10].

Now let's analyze some other boundaries, for example the world records in Athletics[1]. In fact, our organism is very responsive to the FF-attractors and some of these boundaries are insurmountable to anybody.

The world record over 10 km walk is 37 minutes 11 seconds, hold by the Russian athlete Roman Rasskazov in 2000:

$$\ln\left(\frac{10000\,\mathrm{m}/2231\,\mathrm{s}}{c}\right) = -18.02$$

To reach the attractor point [−18], the future world record athlete must walk the 10 km in 2190 seconds = 36 minutes 30 seconds:

$$c \cdot \exp(-18) = 4.56\,\mathrm{m/s} = \frac{10\,\mathrm{km}}{2190\,\mathrm{s}}$$

By the way, this world record walking velocity coincides with the same attractor [−18] we mentioned already in the case of growing traffic jam! The average human walking speed at crosswalks is about 6 km/h = 1.6 m/s. Many people prefer to walk at this speed. Being close to an attractor of stability, this circumstance appears to be natural:

$$\ln\left(\frac{1.6\ \mathrm{m/s}}{c}\right) = -19.05$$

The world record 9.58 seconds over 100 m running was held by the Jamaican athlete Usain Bolt in 2009. Here we can see that his running speed is quite close to the main attractor [−17]:

$$\ln\left(\frac{100\,\mathrm{m}/9.58\,\mathrm{s}}{c}\right) = -17.17$$

Knowing the FF we can affirm that with high probability, nobody will be able to exceed the main attractor [−17] and run over 100 m faster than in 8 seconds:

$$c \cdot \exp(-17) = 12.41\,\mathrm{m/s} = \frac{100\,\mathrm{m}}{8\,\mathrm{s}}$$

[1] List of world records in athletics. www.en.wikipedia.org

The world record 2.45 m in high jump was held by the Cuban athlete Javier Sotomayor:

$$\ln\left(\frac{2.45\ \mathrm{m}}{\lambda_{\mathrm{proton}}}\right) = 36.99$$

This record has been held since 1993. This might demonstrate how unattainable it is. In fact, it is only one centimeter before the main proton attractor point P[37]:

$$\lambda_{\mathrm{proton}} \cdot \exp(37) = 2.46\,\mathrm{m}$$

The attractor P[37] defines a main equipotential surface of the Fundamental Field that affects all processes as well as the growth of the organism. You remember that P[37] defines also the statistical boundary for modern human body height.

Let's analyze also the metric characteristics of some animals. For example, the Peregrine falcon and the Golden eagle can reach flight speeds of 320 km/h close to the main attractor [−15] we know already from the speed limit for ultralight aviation.

Black marlins can swim over large distances with a speed of about 120 km/h. You remember this [−16] attractor speed from the traffic speed limit on European highways.

Greyhounds are the fastest dogs, and have primarily been bred for coursing game and racing. They can hold a running speed close to 74 km/h that coincides with the attractor [−16;−2]. You remember that the speed at high traffic levels on highways fluctuates around this attractor.

The consideration of biophysical characteristics and limitations of the human or animal organism is an important topic in civil engineering and is directly connected with ergonomics. Another not less important topic is the stability of constructions.

Therefore, civil engineering is another field where the knowledge of the FF could be useful. The avoidance of resonance under periodic load in general and seismic stability in particular is and was always an important topic in civil engineering, especially in the Mediterranean region and other areas of permanent seismic activity. Therefore, we can expect that especially large-scale constructions should be responsive to FF-attractors of stability.

Monolithic domes are instructive examples of very high stability. They meet FEMA[1] standards for providing near-absolute protection

[1]Building Codes. FEMA. www.fema.gov

and have a proven ability to survive tornadoes, hurricanes and earthquakes.

In 1991, twenty-eight monolithic domes all of the same size were built in Iraq. Twenty-seven of the domes were grain storages. In addition to these, one more dome was built as a government building in Baghdad. This construction survived a direct hit by a 2300 kg bomb in 2003. The interior of the structure was totally destroyed, but the monolithic dome (inner diameter 117 feet = 35.66 m) itself remained standing except a hole in the top of the dome.[1]

Beginning in 1970, monolithic domes have been built and are in use in virtually every American state and in Canada, Mexico, South America, Europe, Asia, Africa and Australia. Coinciding with the main attractor P[39] diameters of about 36 m are preferred not only in modern constructions, but were favoured in civilizations in antiquity as well. Here are some famous examples of dome constructions from classical antiquity.[2]

The dome of the Pantheon[3] in Rome, an unreinforced monolithic concrete construction with a diameter of 43.7 m and with about 5000 tons of weight, is the archetype of the domes built in the following centuries both in Christian churches and in Muslim mosques.

The 16 massive Corinthian columns supporting the portico weigh 60 tons each. They are 11.8 m = E[31] tall, 1.5 m = E[29] in diameter and brought all the way from Egypt. The hole (oculus) in the top of the dome, 4 m = E[30] in radius, is the only source of light.

The interior space of the Pantheon is completely inside a spheroid with a radius of 21.85 m that is touching the electron stability sub-attractor E[32;−3]:

$$\lambda_{\text{electron}} \cdot \exp\left(32 - \frac{1}{3}\right) = 21.85\,\text{m}$$

The dome of the St. Peter's in Rome has a radius of 21.5 m that touches the proton stability sub-attractor P[39;6]:

$$\lambda_{\text{proton}} \cdot \exp\left(39 + \frac{1}{6}\right) = 21.5\,\text{m}$$

Both radii are in the compression zone of the main attractor P[39] of

[1] Carrison K. Monolithic Mosque in Iraq Still Stands. www.monolithic.org

[2] Como M. Statics of Historic Masonry Constructions. Springer, 2013.

[3] Cinti S. et al. Pantheon. Storia e Futuro / History and Future, Roma, Gangemi Editore, 2007.

proton stability:

$$\lambda_{\text{proton}} \cdot \exp(39) = 18.2\,\text{m}$$

The deviation of the sub-attractors of proton and electron stability is hardly visible in figure 12 because of the logarithmic representation (in the scale of this book the logarithmic deviation of 0.015 appears to be less than 1 mm).

The dome of the Hagia Sophia[1] in Istanbul is of 31.24 m in diameter, so that the radius is touching the sub-attractor E[31;3] of electron stability:

$$\lambda_{\text{electron}} \cdot \exp\left(31 + \frac{1}{3}\right) = 15.65\,\text{m}$$

The Hagia Sophia has survived a big fire in 859 and an earthquake in 869. The dome has collapsed after an earthquake in 989. Due to the earthquakes in 1344 and 1346 a part of the dome and parts of the arch have collapsed and have been repaired.

In Piedmont, Francesco Gallo designed for the drum of the Sanctuary of Vicoforte[2] built by Vitozzi in 1596, one of the largest and complex elliptical domes ever built, with the large diameter being 36 m. As you can see in figure 12, the radii of the Hagia Sophia dome and the Pantheon dome occupy mirror positions in relation to the main attractor P[39] held by the dome of the Sanctuary of Vicoforte.

What do you think: Considering the explicit nonlinearity of the FF and the very sophisticated measurements of proton and electron, could you imagine that this high concurrence of the physical characteristics of antique constructions with the FF happened by chance? Or should we become familiar with the idea that Global Scaling is a rediscovery of a very antique knowledge?

But how and where was this ancient knowledge conserved? May be, it is well exposed in architecture, but we don't see it without Global Scaling glasses?

The German term "Maßwerk" (tracery) brought me on a trail. A tracery consists of geometric patterns and is an important element of Gothic architecture, well exposed in window roses. The term "Maßwerk" derives from "Maß" (measure) and underlines that the geometric patterns contain some metric information. In fact, the diameter of the

[1] Curcic S. Architecture in the Balkans. From Diocletian to Süleyman the Magnificent. Yale University Press, New Haven und London 2010.

[2] Bagliani S. The Architecture and Mechanics of Elliptical Domes. Proceedings of the Third International Congress on Construction History, Cottbus, May 2009.

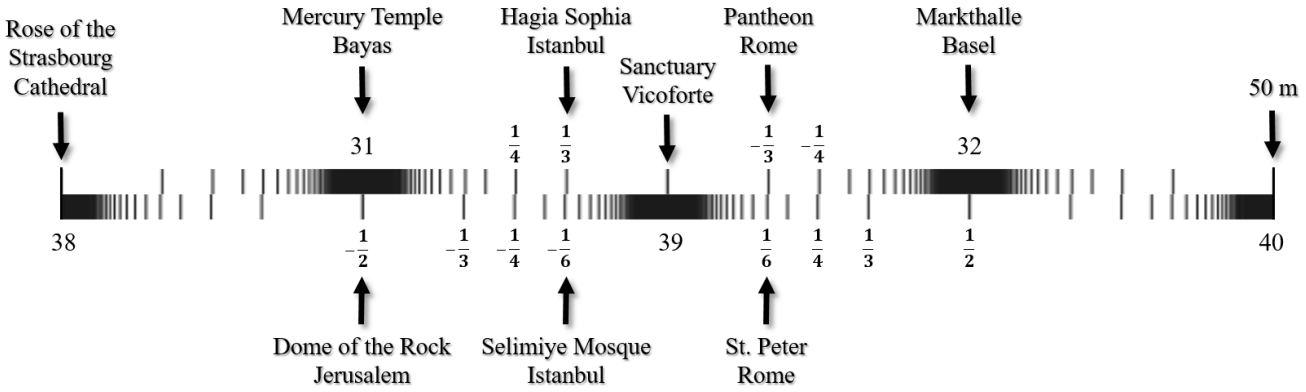

Figure 12: The positions of the radii of some antique domes in the FF calibrated on the Compton wavelengths of the proton (lower FF) $\lambda_{\text{proton}} = 2.103089 \cdot 10^{-16}$ m and of the electron (upper FF) $\lambda_{\text{electron}} = 3,861593 \cdot 10^{-13}$ m.

rose window of the Cathedral of Our Lady of Strasbourg is 13.5 m so that actually its radius coincides perfectly with the main attractor P[38]:

$$\ln\left(\frac{6.7\text{ m}}{\lambda_{\text{proton}}}\right) = 38.00$$

Archeology is based mostly on the interpretation of written documents, such as ancient books and manuscripts, inscriptions on ancient buildings. The main problem is that an inscription can also be made a long time after (even hundreds of years later) a temple was built. And it is well known that at all times, triumphant conquerors rewrote history.

But, how can we know, when and how an ancient construction was built? Andrey Sklyarov[1], a Russian researcher, has shown that we can discover all this by studying the "language of the stones".

Probably, even the Great Pyramid of Giza (GPG) doesn't contain any "chamber of antique knowledge". Rather the pyramid by itself embodies this knowledge. And the giant scale of this construction points to the importance the builders attributed to this knowledge.

I suspect that no explaining script will be found, because only stones can survive time. "Mankind fears Time, but Time fears the Pyramid." Considering the FF as feature of the number continuum, perhaps this Arab proverb refers to its timelessness.

Let's look at the GPG as a message that the builders treated as the most important knowledge they wanted to conserve for all the future generations.

Egyptologists[2] believe that the GPG was built as a tomb for the 4^{th} Dynasty Egyptian pharaoh Khufu (Cheops). The completed design dimensions, as suggested by Petrie's survey and later studies, are estimated to have originally been 280 Egyptian Royal cubits (146.5 m) high by 440 cubits (230.4 m) long at each of the four sides of its base. In this case, the ratio of the perimeter to height of 1760/280 Egyptian Royal cubits would equate to 2π with the well-known approximation of π as 22/7 (p. 13).

However, these are hypotheses and not facts. Furthermore, these estimations are based on a geometric model of an ideal pyramid that does not coincide with the realities of the GPG.

In this book we don't develop hypotheses about what could be the original design of the GPG. Let us analyze only facts in the meaning of

[1] Sklyarov A. The Myth about Flood: calculations and reality. www.lah.ru

[2] Rainer Stadelmann: Die ägyptischen Pyramiden. Vom Ziegelbau zum Weltwunder. Philipp von Zabern Verlag, 1997.

what we can measure and let us assume that the builders did consider the consequences of erosion and other destructive forces.

Actually, the length of the base is not 230 m, but 225 m (like the Pyramide of the Sun in Teotihuacan), and it fits perfectly with the main attractor of stability E[34]:

$$\ln\left(\frac{225\ \mathrm{m}}{\lambda_{\mathrm{electron}}}\right) = 34.00$$

Considering late expansions, removals and repairs, the height[1] of the actual pyramid body is not 146 m, but 137 m like the Chephren pyramid and coincides well with the main attractor P[41]:

$$\ln\left(\frac{137\ \mathrm{m}}{\lambda_{\mathrm{proton}}}\right) = 41.01$$

Considering only realities, the GPG is what it is — a square frustum, like many other pyramids around the world including the great Mexican pyramids. Consequently, the existence of the missing pyramidion could turn out to be a dispensable assumption. If there was some construction on the top or not — we cannot measure it anymore.

The current volume of the GPG is estimated to be 2.5 million cubic meters that coincides with the main attractor P[123]:

$$\ln\left(\frac{2.5\cdot 10^6\ \mathrm{m}^3}{\lambda_{\mathrm{proton}}^3}\right) = 123.02$$

By the way, P[123] = 3P[41]. This means that the volume V of the GPG equals to the cube of its actual height h:

$$V = h^3$$

That's an amazing fact. Here we don't analyze the sizes and the geometry of the chambers, floors and shafts. This will be done in another book. However, from the point of view of Global Scaling, it seems not surprising that the GPG appears as an example of proton and electron stability.

By the way, the Hagia Sophia's giant dome rests on four arches, which are in turn supported by a series of columns and semi-domes. If any of the supports fails, the dome would collapse. To understand

[1] Zahi Hawass. The Treasures of the Pyramids. White Star Publ., Torino (Italy), 2003.

the potential danger to the building, earthquake specialists have built a scale model[1] and performed tests. The team believes that if the model will be damaged by a simulated earthquake, the actual building might be damaged in the same way by a real earthquake.

Talking about modelling, it is a good occasion to learn even more about Global Scaling. One of the principal consequences of the explicit nonlinearity of the FF is that any downscaled real model can not fully simulate the behavior of the original. It is so, because the position in the FF of the model is compellingly different from the position of the original. If the dimension of the original coincides with a main attractor, it is not automatically valid for the model. Consequently, a downscaled model can be damaged by stress while the original will not be affected.

Now you can understand that correctly scaled modelling is not possible without knowledge of the FF. Here arises the question if there are some scaling factors providing for best similarity of the model with the original.

First we can suggest: If the scaling factor of the model is chosen to be an integer potency of Euler's number, some of the model's features will coincide with the original. In this way, if one of the original's measurements coincides with an attractor, the corresponding model's measurement will also coincide with a similar attractor. However, the similarity with the original will be very relative, because it concerns only one physical quantity.

For example, if the radius or height of the original matches with a main attractor and the model is downscaled by a integer potency of Euler's number, other model properties like volume or mass do not automatically match with main attractors.

Naturally, this is valid also for wind tunnel modelling. Only a few objects can be investigated in a wind tunnel without scaling. For airplanes or buildings scaled down models are used. Wind tunnel models of aircraft and spacecraft are designed to extract aerodynamic data for analysis of their full-scale counterparts at specified flight conditions. For example, at the National Transonic Facility at the NASA Langley Research Center, 2.7-percent scale models of the Boeing 777 airplane are mounted to sting support systems for testing at transonic speeds.[2]

[1] Aliberti L. et al. New contributions on the dome of the Pantheon in Rome: comparison between the ideal model and the survey model. The International Archives of the Photogrammetry, Remote Sensing and Spatial Information Sciences, vol. XL-5/W4, 2015.

[2] Chambers J. R. Modeling Flight. The Role of Dynamically Scaled Free-Flight Models in Support of NASA's Aerospace Programs. NASA Publ., 2010.

It isn't difficult to understand that a scaling factor of 0.027 moves the downscaled model in a region of the FF that has nothing in common with the position of the original, because $\ln(0.027) = -3.612$ doesn't match with any main- or first layer attractor like $\pm 1/2, \pm 1/3, \pm 1/4$.

In the consequence, some aerodynamic characteristics of the original can be simulated, but the mechanical behavior including internal resonance can't be tested at all. And so, the test flight of the virgin prototype is still an unavoidable risk, because it will necessarily expose some unpredictable problems which did not appear in the tests of the real model. Therefore, it is always worth to study nature and to learn how the metric characteristics of an established process or structure are distributed in the FF.

Let me return for a moment to the roots of the Fundamental Fractal. Primarily, the FF defines the distribution of frequency ratios which do not support resonance. In this way, any process can avoid destabilizing internal resonance.

In terms of arithmetics, resonance is a question of divisibility without rest. For example, if the duration of two cycles is 3 and 4 seconds respectively, they interact every 12 seconds, because the whole number 12 is divisible by 3 and 4 without rest.

This is valid for all rational numbers being whole number ratios. However, it is not valid for irrational numbers if they are transcendental, because there is no algebraic equation describing them.

Therefore, real transcendental ratios in general exclude resonance, and rational potencies of Euler's number also exclude resonance regarding all derivatives of a process.

It is important to realize that divisibility means the division of a set into parts of equal quantity of elements. Only this multiplicative definition of division corresponds with the meaning of a frequency. For example, $8/4 = 2$ means $8 = 2 + 2 + 2 + 2$. In this case, the frequency is equal to 4 and the duration of one cycle is 2. The same quantity can be divided in non equal parts, for instance $8 = 5 + 3$. In this case it is not possible to define a frequency.

From this point of view, we can understand the origin of the FF in terms of whole numbers and their divisibility and therefore, in terms of sets and their cardinality (number of elements).

In general, any natural number can be interpreted as the cardinality of a set. As we already know, transcendental numbers can be approximated well by rational numbers, and in some cases also by natural numbers. This is also valid for the rational powers of Euler's number. For example, the natural number 20 is a good approximation of e^3, 90

is a good approximation of $e^{4.5}$, and the transcendental number e^9 can be approximated well by the natural number 8103.

Coinciding with attractors of stability, those natural numbers represent cardinalities of stable sets in the sense that these cardinalities prevent any set from destabilizing resonance.

Cardinalities are natural numbers, and the reference unit is the number 1. Therefore, for cardinalities, we write the FF-attractors in square brackets, for example $[9] = e^9$, without E or P.

The interpretation of the FF as distribution of cardinalities of stable sets independent of the nature of the set significantly extends the field of possible applications, including statistics, for example in economy and finances.

As the value of money is represented by real numbers, we can apply the FF also for analyzing the money circulation. In this way we can recognize amounts of higher or lower degree of stability.

Let's analyze the established banknotes where each represents a set (amount) of currency with a fixed cardinality (face value).

Since the face values of the banknotes are adapted to the decimal numeral system, only a few of them coincide with main FF-attractors of stability. Table 4 on the next page shows that only the face values 20 and 50 fulfill this criterion (not counting the trivial case of the face value 1). Which consequences could it have, what do you think?

Provided sufficient liquidity, it could mean that the probability to have banknotes of € 20 is higher than the probability to have banknotes of € 10, for example. This circumstance should affect the quantity of banknotes needed in global circulation. This quantity should significantly depend on the face value.

In fact, statistical data of the Bank of England[1] show that there are nearly three times more £20 bills in circulation than, for example, £10 bills. Instead, the European Central Bank[2] tells that the € 50 bill holds the absolute championship in European domestic circulation.

The US Federal Reserve[3] statistics shows that the $20 bill is the most distributed in domestic circulation. At the same time, the $100 bill is produced produced in incomparably higher quantities, seven times more than the number of $20 bills, but this giant amount of $100 bills doesn't participate in the domestic circulation. How could it be?

[1] Banknote Statistics. Bank of England. 2018, www.bankofengland.co.uk

[2] Banknote Circulation. European Central Bank. 2018, www.ecb.europa.eu

[3] Currency in Circulation: Volume. Currency and Coin Services. Board of Governors of the Federal Reserve System. 2018, www.federalreserve.gov

FACE VALUE C	LN (C)	FF	LN (C) - FF
1	0	[0]	0
2	0.69	[1;−3]	0.03
5	1.61	[2;−3]	-0.06
10	2.30	[2; 3]	-0.03
20	3.08	[3]	0.08
50	3.91	[4]	-0.09
100	4.61	[5;−3]	-0.06
200	5.30	[5; 3]	-0.03
500	6.21	[6; 4]	-0.04

Table 4: Face values of banknotes and their correspondence with FF-attractors. Not counting the trivial case of the face value 1, only the face values 20 and 50 coincide with main attractors.

According to a report in *The Atlantic*[1], $100 bills are a preferred medium of exchange for facilitating clandestine transactions, and for storing illicit and untaxed wealth. These include the illegal trade in drugs, arms and human trafficking as well as amounts of 'unreported' income. An overwhelming majority of the $100 bills comes from the Federal Reserve Cash Office in New York City, which handles the bulk of foreign shipments of US currency. A typical shipment is a pallet containing 640,000 such bills, or $64 million. By the way, this amount is close to the main attractor [18]: $\ln(6.4 \cdot 10^7) = 17.97$.

Indeed, the $100 bill does not coincide with a main attractor of stability and therefore, the quantity of $100 bills should not exceed the quantity of $20 or $50 bills which coincide with main attractors. Consequently, the $100 bill imbalance shows that there is a black market that can destabilize the circulation. In this way, the knowledge about the FF can be applied in economics, and opens the possibility for having information about the financial "state of health".

Now let's come back to mathematics. Talking about divisibility of numbers as resonance condition, we can apply this principle to the logarithms as well.

[1]Matt Phillips. $100 bills make up 80% of all U.S. currency — but why? *The Atlantic*, 21 November 2012, www.theatlantic.com

In general, logarithms are real numbers, and the logarithms of main attractors are whole (integer) numbers. These integer logarithms can be of higher or lower divisibility without rest and therefore, the corresponding attractors have more or less interscalar resonance.

Consequently, a main attractor of higher divisibility, for example P[54], has more interscalar connections with other main attractors than a main attractor of lower divisibility, for example P[51].

Prime number attractors form the basis of interscalar connections because of their non-divisibility. The integer potencies of primes define the position of a main attractor in the interscalar hierarchy. In this sense, square, cubic or higher potencies of prime numbers occupy key positions.

For example, the Sun (p. 31) occupies the main attractor E[49] that is the square of the prime 7. The human zygote (p. 41) occupies the main attractor P[27] that is the cube of 3. By the factor 3 it is connected with the main attractor P[81], the scale of the Galactic Core. The "master planets" Jupiter and Saturn, the "master frequencies" of Theta brain activity (p. 39) and the pituitary "master gland" (hypophysis, p. 41) occupy the main attractor P[54] that is the double cube of 3. The orbit of Venus (p. 30) occupies the main attractor E[54].

Divisible by 12 numbers define local islands of maximum divisibility[1]. For example, the number 60 is divisible by 12, but also by 2, 3, 4, 5, 6, 10, 15, 20, 30 whereas the neighboring numbers 59 and 61 are prime. In consequence, the divisible by 12 attractors of proton and electron stability define channels of maximum interscalar connectivity.

Let us look at some divisible by 12 main attractors and the scales they correspond to. For example, the average size of eukaryotic cells corresponds with the main attractor P[24]. The next divisible by 12 attractor P[36] defines the range of the human body size (pp. 46–47). The average human adult relaxing heart rate (p. 26) corresponds with the main attractor E[48]. The mass of the pineal gland (p. 42) coincides with the attractor E[60], and the weight of the spleen corresponds with the attractor P[60].

Jupiter's surface gravity acceleration (p. 31) meets the main attractor P[72] that defines also the scale of the Oort cloud (0.5 light years), the hypothetic boundary of the solar system. The radius of our Galaxy coincides with the main attractor P[84] and finally, the scale of the observable universe (light horizon) coincides with the attractor P[96].

[1]Shnoll S. E. Cosmophysical factors in stochastic processes. American Research Press, 2012, pp. 400–404

As inherent feature of the number continuum, the FF rules the course of any process and forms all the structures in the universe, regardless of their nature and complexity.

Global Scaling suggests that there is nothing artificial in the universe. All the technology developed by humanity and other civilizations follows the same FF like anything in the universe. Applying Global Scaling, you will see the world with new eyes and explore space and time in a way that hasn't been done before.

Global Scaling leads to an interscalar view of the world that could be a new scientific paradigm. Showing the complex connection of processes at very different scales in the universe, Global Scaling explains mathematically how subatomic and galactic scales are directly related to life as a cosmic phenomenon.

The nature of life isn't competitive struggle. Life is interscalar communication and cooperation.

In the interscalar view, we are not isolated beings, but we are embedded in the solar system, we are an integral part of cosmic life. This is not a poetic phrase, but a scientifically demonstrable fact. This knowledge should be considered in medicine, but also in scholastic education.

Science does not progress because of brilliant minds constantly creating better and better theories. The theory is not the motor of science, rather it is the discovery itself. Nobody can foresee a discovery, it comes unexpectedly and forces the scientist to develop the theory.

Surely, there is a huge field of research where further astonishing discoveries are awaiting us.

Bibliography

1. Müller H. Global Scaling of Planetary Systems. *Progress in Physics*, issue 2, 99–105, 2018.
2. Müller H. Global Scaling of Planetary Atmospheres. *Progress in Physics*, issue 2, 66–70, 2018.
3. Müller H. Quantum Gravity Aspects of Global Scaling and the Seismic Profile of the Earth. *Progress in Physics*, issue 1, 41–45, 2018.
4. Müller H. Gravity as Attractor Effect of Stability Nodes in Chain Systems of Harmonic Quantum Oscillators. *Progress in Physics*, issue 1, 19–23, 2018.
5. Müller H. Astrobiological Aspects of Global Scaling. *Progress in Physics*, issue 1, 3–6, 2018.
6. Müller H. Chain Systems of Harmonic Quantum Oscillators as a Fractal Model of Matter and Global Scaling in Biophysics. *Progress in Physics*, issue 4, 231–233, 2017.
7. Müller H. Global Scaling as Heuristic Model for Search of Additional Planets in the Solar System. *Progress in Physics*, issue 4, 204–206, 2017.
8. Müller H. Scale-Invariant Models of Natural Oscillations in Chain Systems and their Cosmological Significance. *Progress in Physics*, issue 4, 187–197, 2017.
9. Müller H. Scaling of body masses and orbital periods in the Solar System as consequence of gravity interaction elasticity. Abstracts of the XII. International Conference on Gravitation, Astrophysics and Cosmology, dedicated to the centenary of Einstein's General Relativity theory. Moscow, PFUR, 2015.
10. Müller H. Scaling of Moon Masses and Orbital Periods in the Systems of Saturn, Jupiter and Uranus. *Progress in Physics*, issue 2, 165–166, 2015.
11. Müller H. Scaling of Body Masses and Orbital Periods in the Solar System. *Progress in Physics*, issue 2, 133–135, 2015.
12. Müller H. Emergence of Particle Masses in Fractal Scaling Models of Matter. *Progress in Physics*, issue 4, 44–47, 2012.
13. Müller H. Fractal Scaling Models of Natural Oscillations in Chain Systems and the Mass Distribution of Particles. *Progress in Physics*, 2010, issue 3, 61–66.
14. Müller H. Fractal scaling models of natural oscillations in chain systems and the mass distribution of the celestial bodies in the Solar System. *Progress in Physics*, issue 1, 62–66, 2010.
15. Müller H. Fractal Scaling Models of Resonant Oscillations in Chain Systems of Harmonic Oscillators. *Progress in Physics*, issue 2, 72–76, 2009.

16. Müller H. Scaling as Fundamental Property of Natural Oscillations and the Fractal Structure of Space-Time. Foundations of Physics and Geometry. Peoples Friendship University of Russia, 2008 (in Russian).
17. Müller H., Otte R. Verfahren zur Stabilisierung von technischen Prozessen. PCT, WO 2005/071504 A2.
18. Müller H. Superstability as a developmental law of technology. Technology laws and their Applications. Volgograd-Sofia, 1989 (in Russian).
19. Müller H. The general theory of stability and objective evolutionary trends of technology. Applications of developmental and construction laws of technology in CAD. Volgograd, VPI, 1987 (in Russian).
20. Ries A. Qualitative Prediction of Isotope Abundances with the Bipolar Model of Oscillations in a Chain System. *Progress in Physics*, vol. 11, 183–186, 2015.
21. Ries A. A Bipolar Model of Oscillations in a Chain System for Elementary Particle Masses. *Progress in Physics*, issue 4, 20–28, 2012.
22. Ries A. The Radial Electron Density in the Hydrogen Atom and the Model of Oscillations in a Chain System. *Progress in Physics*, issue 3, 29–34, 2012.
23. Ries A., Fook M. Fractal Structure of Nature's Preferred Masses: Application of the Model of Oscillations in a Chain System. *Progress in Physics*, issue 4, 82–89, 2010.
24. Dombrowski K. Rational Numbers Distribution and Resonance. *Progress in Physics*, issue 1, 65–67, 2005.
25. Panchelyuga V. A., Panchelyuga M. S. Resonance and Fractals on the Real Numbers Set. *Progress in Physics*, issue 4, 48–53, 2012.
26. Kolombet V. Macroscopic fluctuations, masses of particles and discrete space-time. *Biofizika.* 1992, vol. 36, 492–499.
27. Shnoll S. E. Cosmophysical factors in stochastic processes. *American Research Press*, 2012.
28. Hilbert D. Über die Transcendenz der Zahlen e und π. *Mathematische Annalen* 43, 216–219, 1893.
29. Max Planck. Über Irreversible Strahlungsvorgänge. In: Sitzungsbericht der Königlich Preußischen Akademie der Wissenschaften. 1899, vol. 1, 479–480.
30. Dirac P. A. M. The cosmological constants. *Nature*, vol. 139, 1937.
31. Markov A. A. Selected work on the continued fraction theory and theory of functions which are minimum divergent from zero. Moscow–Leningrad, 1948.
32. Gantmacher F. R., Krein M. G. Oscillation matrixes, oscillation cores and low oscillations of mechanical systems. Leningrad, 1950.

33. Terskich V. P. The continued fraction method. Leningrad, 1955.
34. Khintchine A.Ya. Continued fractions. *University of Chicago Press*, Chicago, 1964.
35. Skorobogatko V. Ya. The Theory of Branched Continued Fractions and mathematical Applications. Moscow, *Nauka*, 1983.
36. Čislenko L. L. The Structure of the Fauna and Flora in connection with the sizes of the organisms. Moscow, 1981.
37. Schmidt-Nielsen K. Scaling. Why is the animal size so important? *Cambridge University Press*, 1984.
38. Zhirmunsky A. V., Kuzmin V. I. Critical levels in developmental processes of biological systems. Moscow, *Nauka*, 1982.
39. Barenblatt G. I. Scaling. *Cambridge University Press*, 2003.
40. Viehweger R. Understanding the Universe through Global Scaling. Looking at the world with fresh eyes. Quantum Health, Poole, UK, 2012.
41. Viehweger R. Die Welt mit neuen Augen seh'n. Erkenne das Universum durch Global Scaling. Vorwort von Peter Fraser. RABS Verlag, 2010.
42. Marco Bischof. Global Scaling. Das universelle Prinzip der Strukturierung der Welt. *Hagia Chora*, vol. 30, 2008.
43. A Melodia da Criacao. Como o conceito da Escala Global auxilia na busca pelo equilibrio. Entrevista do Hartmut Müller. *QuantumLife*, vol 2, 2015.
44. Global Scaling. *Raum und Zeit*, Special 1, Ehlers Verlag, München, 2007 (in German: Die Basis ganzheitlicher Naturwissenschaft. *Raum & Zeit*, Special Bd. 1, Ehlers Verlag, München, 2004).
45. Global Scaling. Basis eines neuen wissenschaftlichen Weltbildes. Ehlers Verlag, München, 2009.

Acknowledgements

Many have come into this century
to develop arts and sciences,
sow the seeds of a new culture
that will blossom, unexpected, just
when the power is believing it has won.

Giordano Bruno

There are many individuals to whom I am deeply grateful. First of all, I am grateful to my parents who always created best conditions for my studies. With gratitude I remember my high school teachers who enabled me to incorporate some of their lessons.

I am grateful to my country that gave me the possibility to study for free at one of the most famous universities.

I am thankful to Vera Reutova for giving me two beautiful children. Veronika, Erwin and my brother Uwe are always in my heart. They are supporting me and were fighting for me when the power tried to humiliate and destroy me.

I am infinitely grateful to Leili Khosravi. Her love kept me alive when I was locked up for 21 months with 4 prisoners in a completely dark 2 meter small all-metal cell. Leili shares her life with me giving all the light I need to continue my work.

I am grateful to my teachers, colleagues and friends at the Saint Petersburg State University, at the Moscow State University, at the Russian Academy of Sciences and the Volgograd State University of Technology. I am especially grateful to Oleg Kalinin, Simon Shnoll, Victor Panchelyuga and Valery Kolombet, Maria Kondrasheva and Irina Zaychkina, Yury Vladimirov, Dmitry Pawlov, Alexander Beliaev, Alexey Petrukhin and Alexander Polovinkin. They guided my scientific research and made possible the discovery I share with you in this book.

I'm grateful to my graduates and friends: Michael Kauderer and Ulrike Granögger, Ronny and Katja Kircheis and many others who continued to work in the field of Global Scaling, even when it was already defamed by the mass media.

Especially I am grateful to Urs Bühler and Marcel Bauer who founded the HealthBalance Centre in Uzwil, Swizerland and made possible the application of my research in healing and architecture.

I am grateful to Hans-Joachim and Käthe Ehlers, who gave me the possibility to continue my research and to publish it.

I am grateful to my friends in the Community of Living Ethics, especially to Giuseppe Campanella, Marina Bernardi, Gabriella Fini, Paola Bucetti and many others who continuously support my work.

Many thanks to Dmitry Rabounsky, Adreas Ries and Felix Scholkmann who made possible the publication of this book.

About the Author

All truth goes through three stages:
First it seems ridiculous,
then it is fought,
after all, it is self-evident.

Arthur Schopenhauer

Hartmut Müller, born 1954 in Hildburghausen, GDR, studied philosophy and natural sciences at the Saint Petersburg (Leningrad) State University. During a research assistantship, he was also trained in epistemology of scientific research, applied mathematics, particle physics and engineering science.

From 1978 to 1990 Hartmut Müller was teaching philosophy and epistemology of research in engineering sciences at the Volgograd State University of Technology, where he developed Global Scaling methods of analysis and optimization of technology, archived at the Soviet Institute for Scientific and Technical Information.

After his return to Germany, Hartmut Müller became editor of the journal *raum und zeit* of the Ehlers publishing house and cofounded the Global Scaling Research Institute and the non-profit Global Scaling Association for support of research and education.

Hartmut Müller is noted for his public commitment to the non-military application of scientific research. In 2004, for his research and commitment to ethics in science he received the Vernadski medal, the highest recognition of the non-governmental Russian Academic Society. As a result of a slander campaign, he was charged in 2012 with scientific fraud and convicted.

Hartmut Müller has published many scientific papers as well as popular science articles on Global Scaling in particle physics, astrophysics and cosmology, geophysics and biophysics, engineering science and architecture. He also published patents on Global Scaling applications. Today he continues his scientific studies as an independent researcher.

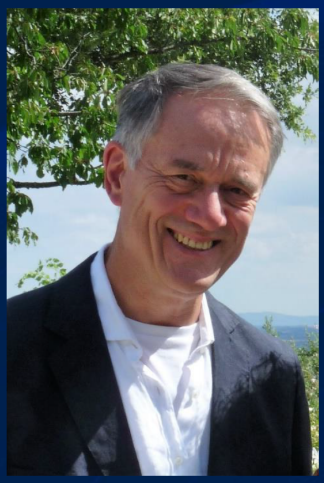

Global Scaling

the fundamentals of interscalar cosmology

by Hartmut Müller

This book is designed as a quick and easy introduction to Interscalar Cosmology that is based on the discovery of a universal law of probably everything – Global Scaling.

The discovery of Global Scaling is the result of an interdisciplinary research that has inspired the author for more than 35 years.

Global Scaling leads to an interscalar view of the world that could become the new scientific paradigm. Showing the complex connection of processes at very different scales in the universe, Global Scaling explains mathematically how subatomic and galactic scales are directly related to life as a cosmic phenomenon.

Global Scaling suggests that there is nothing artificial in the universe. All the technology developed by humanity and other civilizations follows the same fundamental fractal of space-time just like everything else in the universe. It may well be that Global Scaling is the rediscovery of an ancient advanced knowledge.

The reader of this book will find new answers to many questions concerning the nature of the universe and the meaning of life.

A huge field of research with new astonishing discoveries awaits us.

ISBN 978-0-9981894-0-6

9 780998 189406 >

New Heritage Publishers
Brooklyn, New York, 2018